

1 **“Terrigenous material supply to the Peruvian central**
2 **continental shelf (Pisco 14 S) during the last 1100 yr:**
3 **paleoclimatic implications” by F. Briceno Zuluaga et al.**

4 **Answer to Anonymous Referee #1**

5 We are thankful to the anonymous reviewer 1 for the critical and constructive comments, which
6 will help to greatly improve our manuscript. We think that our paper provides a substantial
7 contribution to scientific progress because in this paper we show evidence for a mechanistic
8 understanding of the large changes that occurred in the Eastern Tropical South Pacific during the
9 last millennia. In the new version we will carefully revise the whole manuscript in order to
10 separate the new contribution of this manuscript from the previously published works. In the
11 submitted manuscript we did not explain in detail the methodology and omitted important aspects.
12 In the new version of the manuscript we will explain in more detail the rationale behind our
13 method. We will also include more information about the site and the composite record.

14 **SPECIFIC COMMENTS**

15 Remarks 1: The paper does not present any description of the sedimentary record (no sedimentary
16 log), no description of physical setting of both cores (depth, bathymetry, seismic profile, physical
17 parameters of the water column, : :), no chronological information and no information about how
18 the composite profile as been established. The paper only refers to other papers, but the
19 information is spread over several paper and difficult to synthesize in order to follow the authors
20 rationale.

21 **Response 1:** We agree with the reviewer that we didn't include the full sedimentological
22 characteristics of the cores used in this study since they have been fully described in other papers
23 as in Gutierrez et al., 2006; Sifeddine et al., 2008 and Salvattecí et al., 2014) for core B06. In the
24 revised version we will add more information about the site and the composite record as suggested
25 by the reviewer.

26 Remarks 2: The paper should also explain what are the phenomenons behind the formation
27 of laminations.

28 **Response 2:** The Pisco continental sediments are characterized by a succession of darkness and
29 lightness laminae. This laminae structure is related to a complex interplay of factors including
30 temporal variations in the quantity of terrigenous sediments supplied to the shelf by rivers and
31 then by bottom currents as well as variations in the fluxes of siliceous and organic components to
32 the sediment floor, which in turn are a function of upwelling-driven productivity and dissolution
33 in the water column (Brodie and Kemp, 1994, Salvattecí et al., 2014 Mar Geo). Finally, the
34 existence of strong oxygen minimum zone (OMZ) inhibiting bioturbation (Gutiérrez et al., 2006)
35 and low currents actions allow the hemipelagic sedimentation (Suess et al., 1987). We will add in
36 the revised version of the manuscript more relevant information about the formation of
37 laminations and how we can use them to assemble composite records.

39 Remarks 3: Moreover, it is impossible to find a description of core G-10 in the Salvattecí et al
40 2014 (Clim Past) from the reference list.

41 **Response 3:** The stratigraphic approach, sediment sub-sampling, age model of core G10 are
42 presented in the supplementary data (SM1, SM2 and SM3) of Salvattecí et al., 2014b (Clim. Past).
43 In the revised version of the manuscript we will include more information about core G10 and
44 how the composite record was assembled.

45 Remarks 4: However, I found another paper by Salvattecí et al. 2014 in Marine Geology,
46 describing the stratigraphy of core B-6, but there is no mention of G-10 in this paper. This latter
47 paper shows that the link between two cores in this setting is difficult to do because of slumps
48 induced by earthquakes. It is therefore critical to explain how the composite section has been built
49 for this paper, and have a comprehensive description of the sedimentary sequence and the
50 geological setting. It raises some concerns about the reproducibility and the traceability of results.

51 **Response 4:** We agree with the reviewer that is critical to explain how the composite record was
52 assembled. We will do this in detail in the revised version. The paper by Salvattecí et al., Mar
53 Geo, shows that it is difficult to establish the link between cores but it has been done for several
54 cores off Pisco including B6 and G10 (see figure SM1 in Salvattecí et al CPD supplementary
55 material). The paper published by Salvattecí et al (Mar geology) raises concerns reproducibility
56 of the results only if a careful sediment logical description of the cores by X-ray images means is
57 not done. For example two cores collected 300 km show the same centennial-scale variability
58 during the last 700 years (Gutiérrez et al. 2009). These two cores (one of them is B6) have
59 independent chronologies based on several ^{210}Pb and ^{241}Am data points, several ^{14}C ages, and
60 the identification of sedimentological structures by X-ray images.

61 Remarks 5: Another problem is that authors are mentioning a southward redistribution of river
62 sediments because of currents, a feature that is indeed credible.

63 However, authors should at least discuss the possibility of countourite that could occur in this
64 kind of settings, i.e. continental slope. This is critical, because countourites are capable of
65 moving/depositing sediment such as coarse silts and fine sands. Sedimentological analyses
66 demonstrate that slope-parallel currents lead to winnowing of fine particles and (re)deposition of
67 allochthonous material, which alters the grain-size populations, (see for instance Mulder et al.,
68 2013) and the paleoclimatic reconstruction that are performed using these kind of sediments (for
69 instance Keigwin, L. D., and M. A. Schlegel (2002)).

70 **Response 5:** The formation of countourite is one of characteristic off north Peru but not in the
71 Pisco area because Reinhardt et al., 2002; Suess et al., 1987 and Gutiérrez et al., 2006 have
72 described the sedimentary facies in the Peruvian shelf as well as the role of currents in the erosion
73 and redistribution processes over the Peruvian continental shelf. These works have showed that
74 high resolutions sediment record should be present only in specific localities of the continental
75 margin (high rate sedimentation zones). First, Suess et al, (1987) described the formation of two
76 sedimentary characteristic facies between $6 - 10^\circ\text{S}$ and $11 - 16^\circ\text{S}$. The first area ($6 - 10^\circ\text{S}$,
77 Salaverry basin) is characterized by the absence of sediment accumulation due to strong
78 undercurrents. This area could be a good candidate for studying the contourites (if any) and the
79 undercurrents effects considering the diagnostic criteria described in Rebesco et al., (2014). The
80 second area ($11 - 16^\circ\text{S}$, Lima Basin) is characterized by lens shape of depositional center of
81 organic-rich mud facies favored by the oceanographic dynamic within the continental shelf, such
82 as the position and velocity of the southward poleward current (Gutiérrez et al., 2006; Reinhardt
83 et al., 2002; Suess et al., 1987). In addition to the works quoted above, high resolution profile was

84 obtained with ecosounder Bathymetry 2000P during the "Paleomap 2006" cruise. The identified upper
85 mud lenses are characterized by fine grain size, diatomaceous, hemiplegic mud and high organic
86 carbon and the absence of erosive and bioturbation processes. We will add more information
87 about this in the revised version of the manuscript.

88 **Remarks 6:** The grain size distributions presented here also are quite similar to the grain-size
89 distributions smaller than 200 μm found in other countourites. This is a serious problem because
90 the technique used here does not include the fraction $> 200 \mu\text{m}$. Therefore, it should be essential
91 to provide the reader with quantities of sediment that were removed from the grain-size analysis
92 because of this filtering. Authors should also justify why they used the Flow Particle Image
93 Analyzer technology rather than regular techniques that are capable of analyzing the full size
94 range of sediments, and demonstrate this is not important for the interpretation of the results.

95 **Response 6:** We apologize for this misunderstanding, we forgot to mention in the submitted
96 version that particles coarser than 200 μm were never found in any samples after sieving. That
97 means that the sediment samples do not contain such coarse particles, and that the grain-size
98 distributions displayed in this study well represent the whole samples. As a consequence, the use
99 of the Flow Particle Image Analyzer (with its restriction on measurable size ranges) has no
100 consequence on the results and their interpretation. Moreover, such grain-size analyzer allows us
101 to obtain images of all the detected particles and therefore, to check the efficiency of the chemical
102 pretreatment of the samples, which is an important step in the grain-size analysis.

103 TECHNICAL COMMENTS

104 L61: GSD is not mixed since laminations are preserved, and I therefore suggest the following
105 wording: "Grain size distribution in laminated marine sediments may indicate different sources
106 and/or deposition processes, expressed as polymodal distributions.

107 **Response:** Thank you for the suggestion; we will modify this sentence as suggested.

108 L65: I suggest the following: "(: :) identifying the different sedimentary processes and the past
109 environmental conditions behind them (: :)"

110 **Response:** Agree, we will change the sentence.

111 L96-97: I'm sorry, but there is little about the sedimentary processes *sensu stricto* in the paper.
112 For instance, authors are not really explaining what type of current/process leads to deposition of
113 riverine material.

114 **Response:** In fact, there is a wealth of information on sedimentary processes on the continental
115 shelf explaining the dispersion and deposition that were eventually cited in the document.
116 Optionally we could written a brief summary indicating works such as Reinhardt et al., (2002);
117 Smith, (1983); Suess et al., (1987).

118 L101-111: The information presented here is not sufficient to have a self-sustaining paper. A lot
119 more information about the cores and the site should be included in the paper.

120 **Response:** We agree with this suggestion and will include more information about the study area,
121 the cores, the composite record to have a self-sustaining paper.

122 L112-121: I understand what you are aiming for, but the practical explanations remains unclear.
123 Please rephrase this section.

124 **Response:** We will rephrase this part for a better comprehension.

125 L123-127: The sample thickness is missing. It is important because it would provide an idea of
126 the number of laminations included in each analysis. It should be also a good idea to provide the
127 variation of the number of laminations through time.

128 **Response:** Sample thickness in core B6 ranges from 0.5 cm to 1.0 cm, and usually includes 2-3
129 laminae in core G10 each sample is 1 cm thick and usually include 3-4 laminae. In our manuscript
130 we are not focusing on sub-decadal or decadal-scale time series. We focus on centennial-scale
131 changes in terrigenous input and thus we were not interested at the laminae scale variations that
132 will be an interesting work especially for the last 100 years of the record.

133 L127-129: It is essential to provide the reader with quantities of sediment that were removed from
134 the grain-size analysis because of this filtering. The interpretation of the data highly depends on
135 that.

136 **Response:** As mentioned above (Response 5), this information is unfortunately missing. We will
137 add it in the text in section 2.1 - Grain size analyses as follows: "In practice, particles larger than
138 200 µm had never been encountered in any samples"

139 We apologize for this misunderstanding, we forgot to mention in the submitted version that particles coarser
140 than 200 µm were never found in any samples after sieving. We processed the whole sample, nothing
141 was removed from the sample. We will modify this accordingly in the revised version of the
142 manuscript.

143 L185-186: Sun et al. (2002) indeed write that, but in the frame of loess sediments. The exact
144 citation is: "In loess deposits, the wide size range of the fine component and the low degree of
145 sorting suggest that they are slowly and continuously deposited throughout the year. This is
146 not applicable here.

147 **Response:** This assumption is applicable too for our scenario because the assumption that the
148 fluvial input particles is a slowly and continuously deposited throughout the year.

149 L189: What are these favorable erosional soil properties? Are they consistent with the situation
150 here?

151 **Response:** favorable conditions are for erosion are: lack of vegetation, low threshold friction
152 velocity, surface roughness and low soil moisture. For more details, see Iversen and White, (1982)
153 and Marticorena and Bergametti, (1995). Such conditions prevail in the studied area since the
154 central coastal Peru consists of a sandy desert area characterized by no rain, a lack of vegetation
155 and persistent wind (see, for instance, Haney and Grolier, 1991). This will be better addressed in
156 the paper.

157 *Haney, E.M. and M.J. Grolier, Geologic map of major Quaternary aeolian features, northern and central*
158 *coastal Peru, IMAP 2162, USGS Publications Warehouse, 1991*

159 L192: The sample that is the most influenced by wind in Stuut et al. 2007 (core GeoB7108) has
160 a mode that is 400µm, something that the authors in this study would have missed because of the
161 technique used. Moreover, the grain-size analyses interpreted by Stuut et al (2007) were only
162 described for the samples from water depths >1000 m. Since cores are collected at much shallower
163 depths in this study is the Stuut et al (2007) interpretation still valid? Again, this is critical to
164 address this issue to support your interpretation.

165 **Response:** As already mentioned, we didn't miss any size-mode and our samples do not contain
166 any particles coarser than those detected. On the other hand Stuut, et al (2007) related the presents

167 of typical distribution of wind-blown transport near to ~80µm (~29°S North of Chile) which is
168 consistent with our results. In this case the relationship between distance and wind force and
169 conditions of sedimentation is more important than depth.

170 L193: Flores-Aqueveque et al., 2015; these authors are mentioning particle >100 µm and actually
171 in their figure 7, they measured grains up to 400µm, which would not have been measured by the
172 grain-size technique used in this study.

173 **Response:** We didn't miss any size-mode and our samples do not contain any particles coarser than those
174 detected, we did not explain in detail in the submitted manuscript but will do in the revised version.
175 Moreover, there is no Figure 7 in Flores-Aqueveque et al., 2015. So, we don't know to which
176 paper the reviewer is referring.

177 L197-198: Is this last sentence really useful?

178 **Response:** Maybe not. Thus, this part could be rewritten to better understanding of the reader

179 L199-201: Contourite and hyperpycnal flows can transport these coarse grains. Moreover, some
180 of the co-authors of this paper reported the presence of slumps in this area in another paper;
181 slumps can transport coarse grains. Authors should carefully and comprehensively argue that
182 these phenomena do not affect sedimentation here, otherwise their interpretation falls apart.

183 **Response:** Suess et al, (1987) described the formation of two sedimentary characteristic
184 sedimentary facies between 6 – 10°S and 11 – 16°S. The first area (6 – 10°S, Salaverry basin) is
185 characterized by the absence of sediment accumulation due to strong undercurrents. This area
186 could be a good candidate for studying the contourites (if any) and the undercurrents effects
187 considering the diagnostic criteria described in Rebesco et al., (2014). The second area (11 – 16°S,
188 Lima Basin) is characterized by lens shape of depositional center of organic-rich mud facies
189 favored by the oceanographic dynamic within the continental shelf, such as the position and
190 velocity of the southward poleward current (Gutiérrez et al., 2006; Reinhardt et al., 2002; Suess
191 et al., 1987). This should be explaining in details in the new version of the paper.

192 L219-220: McCave writes in the abstract: “We cannot use size distributions to distinguish the
193 nature of the currents.

194 **Response:** In fact, the aim of this paper is not to see the nature of the currents but particles sources.

195 L230-231: Again, the composite record should be described in this paper.

196 **Response:** We agree with the reviewer, more details about the composite record will be added to
197 the revised version of the manuscript

198 **Bibliography**

199 Gutiérrez, D., Sifeddine, A., Reyss, J., Vargas, G., Velasco, F., Salvattecchi, R., Ferreira, V., Ortlieb,
200 L., Field, D., Baumgartner, T., Boussafir, M., Boucher, H., Valdes, J., Marinovic, L., Soler, P.
201 and Tapia, P.: Anoxic sediments off Central Peru record interannual to multidecadal changes of
202 climate and upwelling ecosystem during the last two centuries., *Adv. Geosci.*, 6, 119–125, 2006.

203 Iversen, J. D. and White, B. R.: Saltation threshold on Earth, Mars and Venus, *Sedimentology*,
204 29, 111–119, doi:10.1111/j.1365-3091.1982.tb01713.x, 1982.

205 Marticorena, B. and Bergametti, G.: Modeling the atmospheric dust cycle: 1. Design of a soil-
206 derived dust emission scheme, *J. Geophys. Res.*, 100(D8), 16415, doi:10.1029/95JD00690, 1995.

207 Rebesco, M., Hernández-Molina, F. J., Van Rooij, D. and Wåhlin, A.: Contourites and associated

208 sediments controlled by deep-water circulation processes: State-of-the-art and future
209 considerations, *Mar. Geol.*, 352, 111–154, doi:10.1016/j.margeo.2014.03.011, 2014.

210 Reinhardt, L., Kudrass, H., Lückge, A., Wiedicke, M., Wunderlich, J. and Wendt, G.: High-
211 resolution sediment echosounding off Peru Late Quaternary depositional sequences and
212 sedimentary structures of a current-dominated shelf, *Mar. Geophys. Res.*, 23(1980), 335–351,
213 2002.

214 Smith, R. L.: Circulation patterns in upwelling regimes, *Coast. upwelling*, 13–35, 1983.

215 Suess, E., Kulm, L. D. and Killingley, J. S.: Coastal upwelling and a history of organic-rich
216 mudstone deposition off Peru, *Geol. Soc. London, Spec. Publ.*, 26(1), 181–197,
217 doi:10.1144/GSL.SP.1987.026.01.11, 1987.

218

219 **Answer to Anonymous Referee #2**

220 We are very grateful for the quite thoughtful anonymous reviewer 2. Clearly, the reviewer spent
221 much time and effort as put on the part of the reviewer and we appreciate his/her comments very
222 much, which will support to greatly improve our manuscript.

223 **General comments:**

224 Remarks 1: The manuscript presented by Zuluaga et al. use grain size distribution of two
225 laminated sediment cores collected off Peru to reconstruct terrigenous material supply to the
226 Peruvian shelf over the last ~ 1100 yr at high resolution. Although the manuscript falls within the
227 scope of CP, to my knowledge, it does not add novel information about the past climate of the
228 area.

229 **Response:** We think that our paper provides a substantial contribution to scientific progress
230 because we show new evidence for a mechanistic understanding of the large changes of
231 terrigenous input (fluvial vs Aeolian transport) that occurred in the Eastern Tropical South Pacific
232 during the last millennia. In fact, our data of grain-size distribution provides an accurate and
233 specific proxy of fluvial input changes which confirms the previous findings by Rein et al. (2004),
234 Sifeddine et al. (2008) and Gutierrez et al. (2009) using mineralogical proxies. Moreover, we
235 present new evidence for the variability of wind intensity and then atmospheric circulation in a
236 temporal scale. We also provide an accurate proxy of runoff linked to the ENSO-like variability.
237 In the new version we will carefully revise the whole manuscript in order to separate the new
238 contribution of this manuscript from the previously published works and highlight their
239 importance.

240 Remarks 2: Additionally, the manuscript lacks description of the sediments (at least a short
241 lithological summary for both cores; lamination throughout? in part?), collection sites and
242 detailed composite chronology. Moreover, the interpretation of grain-size data seems to be
243 oversimplified for a continental shelf area that is geologically not that simple. More information
244 on the physical setting of coring sites and transport mechanisms of particles from the continent
245 needs to be provided.

246 **Response:** We agree with the reviewer that we didn't include the full sedimentological
247 characteristics of the cores used in this study. As it was discussed (with Referee 1) that these
248 characteristics have been fully described in other papers such as Gutierrez et al., 2006; Sifeddine
249 et al., 2008 and Salvatelli et al., 2014 for core B06. However, in the revised version we will add

250 more information about the sedimentological characteristics as suggested by the reviewers. In
251 the new version of the manuscript we will explain in more detail the rationale behind our method
252 and explain in detail each aspect. Also, as it was discussed with the Referee 1, we can make a
253 small overview of the most important oceanographic and sedimentary characteristics in finding a
254 better understanding of the properties of the records.

255 In the full review and interactive discussion, the referees and other interested members of the
256 scientific community are asked to take into account all of the following aspects:

257 1. Does the paper address relevant scientific questions within the scope of CP? YES

258 2. Does the paper present novel concepts, ideas, tools, or data? NOT REALLY

259 **Response:** We agree with the reviewer that is better explain the scope of the paper and mention
260 that in fact there are no works of the sedimentological dynamic input as proxy of the behavior of
261 the atmospheric variability i.e. precipitation (runoff) and continental wind intensity in high
262 resolution in the eastern of Peru. Besides, the proxy we used, disentangling the data showed the
263 evolution of the climatology mechanism (ITCZ-SPSH) in response of the principal climate
264 periods and its relationship with both wind intensity and fluvial input variability. Important
265 mechanisms for understanding the atmospheric-ocean dynamic in this area are relevant for the
266 Humboldt upwelling system dynamic and the relationship with the ENSO conditions. In the new
267 version we will carefully revise the whole manuscript in order to underline the new contribution
268 from the previously published works. For the first time the origin and the mechanism of transport
269 of the terrigenous materials in the continental shelf are elucidated and deciphered as direct
270 indicators of the behavior of the atmospheric variability i.e. precipitation (runoff) and continental
271 wind intensity.

272 3. Are substantial conclusions reached? NOT REALLY

273 **Response:** In the new version we will pay attention in guide better each one of the conclusions
274 and its relevant importance. We think that our paper provides a substantial contribution to
275 scientific progress of the paleoclimatology occurred in the Eastern Topical South Pacific during
276 the last millennia.

277 4. Are the scientific methods and assumptions valid and clearly outlined? NOT REALLY

278 **Response:** The methodology used in this work (the Flow Particle Image Analyzer technology)
279 has several advantages: First, each of the particles can be seen in each sample, which assures the
280 analysis of mineral particles only, assessing the chemical attack efficiency and offering the
281 possibility of elimination of the non-lithological particles. Images may be used to identify the
282 origin of particles by their optical characteristics such as the case of black carbon (Flores-
283 aqueveque et al., 2014). Moreover, if one ignores the images, this method provides grain-size
284 information comparable to that obtained with a classic laser granulometer methodology. Finally,
285 in the aim to indicate the different sources and/or deposition processes, several works use the
286 deconvoluted gran size with success as Gomes et al., 1990; Prins and Weltje, 2012; Stuu et al.,
287 2002, 2007; Weltje and Prins, 2003.

288 5. Are the results sufficient to support the interpretations and conclusions? It is not a self-
289 sustaining paper

290 **Response:** Previous sedimentological studies in the upwelling area as Böning and Brumsack,
291 2004; Gutiérrez et al., 2006, 2008, 2011; Reinhardt et al., 2002; Salvattecí et al., 2012, 2013;
292 Sifeddine et al., 2008; Suess et al., 1987 and others, showed that these markers can be used to
293 reconstruct paleoceanographic/paleoclimatological variability. This area presents laminated
294 sediments material without bioturbation and low currents erosion action (Gutiérrez et al., 2006;
295 Reinhardt et al., 2002; Suess et al., 1987) which represents an area suitable for
296 paleoenvironmental studies. Based on these studies, we applied a new grain-size proxy used as a
297 marker of terrigenous input as used by Flores-Aqueveque (2015). The grain-size distribution is
298 an accurate proxy to reconstruct aeolian transport as used in (Mulitza et al., 2010; Prins and
299 Weltje, 2012; Stuut et al., 2002, 2007; Sun et al., 2002; Weltje and Prins, 2003). We will include
300 more information about the study area, the cores, and the composite record to have a self-
301 sustaining paper. We agree with the reviewer in the fact of including sedimentological
302 characteristics section of the cores used in this study although this has been done in other papers
303 (i.e. Gutierrez et al., 2006; Sifeddine et al., 2008 and Salvattecí et al., 2014).

304 6. Is the description of experiments and calculations sufficiently complete and precise to allow
305 their reproduction by fellow scientists (traceability of results)? NOT COMPLETELY; chronology
306 not given; full range of grain-size not given.

307 **Response:** These two cores have independent chronologies based on several ²¹⁰Pb and ²⁴¹Am
308 data points, several ¹⁴C ages, and the identification of sedimentological structures by X-ray
309 images. Although this data was published in other works, we will show the chronological models
310 in the supplementary material. On the other hand, we must apologize for forgetting to mention
311 that particles coarser than 200 μm were never found in any samples. In fact particles >130 μm
312 were very rare to find. As consequence our data, represent the full range of the grain size.

313 7. Do the authors give proper credit to related work and clearly indicate their own new/original
314 contribution? YES

315 8. Does the title clearly reflect the contents of the paper? YES

316 9. Does the abstract provide a concise and complete summary? YES

317 10. Is the overall presentation well structured and clear? YES

318 11. Is the language fluent and precise? NEEDS SOME WORK

319 **Response:** Thank you for the suggestion; we will work in this item as suggested.

320 12. Are mathematical formulae, symbols, abbreviations, and units correctly defined and used?
321 YES

322 13. Should any parts of the paper (text, formulae, figures, tables) be clarified, reduced, combined,
323 or eliminated? SEE BELOW, SPECIFIC COMMENTS

324 14. Are the number and quality of references appropriate? YES, although there seems to be too
325 many references, and some are not relevant.

326 15. Is the amount and quality of supplementary material appropriate? NO. The suppl. Material
327 should include the age model of both cores B040506 and G10-GC-01, and especially details on
328 how the composite record was build. This is a critical point.

329 **Response:** We agree with this suggestion and as appointed before we will include this information
330 in the supplementary material looking for a better understanding of the manuscript. On the other
331 hand, more details about the composite record will be added to the revised version of the
332 manuscript.

333 **Specific comments:**

334 Although the authors present new data (i.e. grain-size) for the Pisco shelf area, I have 3 main
335 concerns that need to be addressed before this manuscript can be considered for publication:

336 1) Physical setting of the collection sites needs to be given as well as a summarized sediment
337 description.

338 The manuscript lacks presentation of the sampling sites with respect to processes (other than
339 eolian input) that may affect the transport of particles from the continent to the ocean (e.g., strong
340 or weak bottom currents?, erosional processes, slumps/earthquakes, etc.).

341 Moreover, the Salvattecí et al. (2014 in CP) paper in its supplementary information reveals 2
342 slumps in core G-10, some clearly laminated sections and several banded intervals. X-radiographs
343 of nine cores are shown in this publication (including G-10 and B-06), all of them showing
344 intervals with slumps.

345 Citing Salvattecí et al. (2014 in Marine Geology vol 357): "... two possible mechanisms can
346 explain the presence of the homogeneous sediments: slumps triggered by earthquakes and
347 sediment instabilities, and/or sediment transported by strong bottom currents". ... "Another
348 mechanism that can be responsible for the re-deposition of sediment from upslope in some
349 portions of the cores could be related to changes in the intensity of the Poleward Undercurrent
350 which is stronger during El Niño events". ... "All the cores evaluated in the present work show
351 discontinuities and the addition of previously deposited material". With so many factors at play,
352 isn't the interpretation of grain size in this manuscript somewhat oversimplified? By the way, I
353 could not find the reference to the frequently cited Salvattecí et al. (2014) in the reference list.

354 **Response:** We agree with the referee in this point and in the new version of the manuscript we
355 will write a section describing the sedimentological and oceanographic features that allow the
356 hemipelagic sedimentation and the formation of the laminated sediments in the Pisco continental
357 shelf. These features have been previously addressed deeply by Gutierrez et al., (2006); Reinhardt
358 et al., (2002); Saukel et al., (2011); Scheidegger and Krissek, (1982); Smith, (1983); Suess et al.,
359 (1987) and we can make a description in the new version of the paper. Regarding the comment
360 about the difficulties to link two sediment cores, the slump in different sediment cores in fact
361 exist. Differences between records do not necessarily represent losses as not direct evidence of
362 discontinuities was found, and maybe it is product of differences in the sedimentation rate as was
363 appointed by (Salvattecí et al., 2014). Nevertheless we can reconstruct historical record using
364 different cores of the same area (Pisco mud lens) as was the case here. The paper by Salvattecí et
365 al., Mar Geo, shows that it is difficult to establish the link between cores but it has been done for
366 several cores off Pisco including B6 and G10 (see figure SM1 in Salvattecí et al CPD
367 supplementary material). The distribution and deposition of particles is consistent in both
368 sediments cores. In this work we did not consider that slumps in the record for analysis and for
369 the temporal windows showed here processes as bottom currents erosions appear to be negligible.
370 Indeed, the sediment section chosen here to complete the record (S5 in the core G10) has no
371 hiatuses and cover the MCA period. We will mark in the figures and include additional material

372 about how the composite record was assembled. Finally we will include the correct reference for
373 Salvattecchi et al. (2014) in the final version.

374 2) Chronology. Detailed chronology for both cores used in this manuscript needs to be included
375 as well as an explanation on how the composite record has been built. Given the issues raised in
376 (1), this is critical! Please add X-radiographs of the cores and the composite, a table/fig. with the
377 Pb210 and C-14 data, and the overlap/match between both cores.

378 **Response:** We agree with the reviewer that it is critical to explain how the composite record was
379 assembled. We will do this in detail in the revised version. These two cores have independent
380 chronologies based on several ²¹⁰Pb and ²⁴¹Am data points, several ¹⁴C ages, and the
381 identification of sedimentological structures by X-ray images. In the new version we will include
382 a table or figure with the chronological information.

383 3) Grain-size Analysis. a) Authors should state the advantages/disadvantages of using the chosen
384 method (Flow Particle Image Analyzer) over other techniques. This goes in hand with the
385 question: a) Is the >200 microns fraction not important off Peru, on a setting such as the
386 continental shelf? If so, please tell us why.

387 **Response:** We apologize for this misunderstanding, we forgot to mention in the submitted version
388 that particles coarser than 200 µm were never found in any samples after sieving. That means that
389 the sediment samples do not contain such coarse particles, and that the grain-size distributions
390 displayed in this study well represent the whole samples. On the other hand the Flow Particle
391 Image Analyzer technology has several advantages: First each of the particles can be seen in each
392 sample, which assures the analysis of mineral particles only, assessing the chemical attack
393 efficiency and offering the possibility of eliminate the non-lithological particles. Images may be
394 used to identify the origin of particles by their optical characteristics such as the case of black
395 carbon (Flores-aqueveque et al., 2014). Finally, if the images are to be ignored, this method
396 provides size information comparable to that obtained with a classic laser granulometer
397 methodology.

398 b) Removal of opal. Have the authors checked that all opal was really removed? What is the opal
399 content in Pisco sediments? (I believe these are sediments loaded with diatoms). Over the years
400 it has become more and more evident that the removal of all opal from a sample is not an easy
401 task. Please add a sentence or two about this issue in the methods section, making sure that the
402 methodology employed has removed all opal from each sample.

403 **Response** Using the Flow Particle Image Analyzer technology allows us to capture images of all
404 the particles passing through the cell measurement. We observed that opal had been fully removed
405 from all the analyzed samples, which confirm the efficiency of the pretreatments we used.

406 **Bibliography.**

407 Böning, P. and Brumsack, H.: Geochemistry of Peruvian near-surface sediments, *Geochim.*
408 *Cosmochim. Acta*, 68(21), 4429–4451, doi:10.1016/j.gca.2004.04.027, 2004.

409 Flores-aqueveque, V., Caquineau, S., Alfaro, S. and Valde, J.: Using Image-based size analysis
410 for determining the size distribution and flux of eolian particles sampled in coastal northern Chile
411 (23°S), *J. Sediment. Res.*, 84, 238–244, 2014.

412 Gomes, L., Bergametti, G., Dulac, F. and Ezat, U.: Assessing the actual size distribution of
413 atmospheric aerosols collected with a cascade impactor, *J. Aerosol Sci.*, 21(1), 47–59,
414 doi:10.1016/0021-8502(90)90022-P, 1990.

415 Gutiérrez, D., Bouloubassi, I., Sifeddine, A., Purca, S., Goubanova, K., Graco, M., Field, D.,
416 Méjanelle, L., Velazco, F., Lorre, A., Salvattecí, R., Quispe, D., Vargas, G., Dewitte, B. and
417 Ortlieb, L.: Coastal cooling and increased productivity in the main upwelling zone off Peru since
418 the mid-twentieth century, *Geophys. Res. Lett.*, 38(7), 1–6, doi:10.1029/2010GL046324, 2011.

419 Gutiérrez, D., Sifeddine, A., Field, D., Ortlieb, L., Vargas, G., Chaves, F., Velazco, F., Ferreira,
420 V., Tapia, P., Salvattecí, R., Boucher, H., Morales, M. C., Valdes, J., Reyss, J., Campusano, A.,
421 Boussafir, M., Mandeng-Yogo, M., Garcia, M. and Baumgartner, T.: Rapid reorganization in
422 ocean biogeochemistry off Peru towards the end of the Little Ice Age, *Biogeosciences*, 5(August),
423 835–848, 2008.

424 Gutiérrez, D., Sifeddine, A., Reyss, J., Vargas, G., Velasco, F., Salvattecí, R., Ferreira, V., Ortlieb,
425 L., Field, D., Baumgartner, T., Boussafir, M., Boucher, H., Valdes, J., Marinovic, L., Soler, P.
426 and Tapia, P.: Anoxic sediments off Central Peru record interannual to multidecadal changes of
427 climate and upwelling ecosystem during the last two centuries., *Adv. Geosci.*, 6, 119–125, 2006.

428 Gutierrez, D., Sifeddine, A., Reyss, J., Vargas, G., Velasco, F., Salvattecí, R., Ferreira, V., Ortlieb,
429 L., Field, D., Baumgartner, T., Boussafir, M., Boucher, H., Valdes, J., Marinovic, L., Soler, P.,
430 Tapia, P. and Gutiérrez, D.: Anoxic sediments off Central Peru record interannual to multidecadal
431 changes of climate and upwelling ecosystem during the last two centuries, *Adv. Geosci.*, 6, 119–
432 125, 2006.

433 Mülitz, S., Heslop, D., Pittauerova, D., Fischer, H. W., Meyer, I., Stuut, J.-B., Zabel, M.,
434 Mollenhauer, G., Collins, J. a, Kuhnert, H. and Schulz, M.: Increase in African dust flux at the
435 onset of commercial agriculture in the Sahel region., *Nature*, 466(7303), 226–8,
436 doi:10.1038/nature09213, 2010.

437 Prins, M. A. and Weltje, G. J.: End-member modeling of siliciclastic grain-size distributions: The
438 late Quaternary record of aeolian and fluvial sediment supply to the Arabian Sea and its
439 paleoclimatic significance, *SEPM (Society Sediment. Geol.)*, 62, 91–111, 2012.

440 Reinhardt, L., Kudrass, H., Lückge, A., Wiedicke, M., Wunderlich, J. and Wendt, G.: High-
441 resolution sediment echosounding off Peru Late Quaternary depositional sequences and
442 sedimentary structures of a current-dominated shelf, *Mar. Geophys. Res.*, 23(1980), 335–351,
443 2002.

444 Salvattecí, R., Field, D. B., Baumgartner, T., Ferreira, V. and Gutierrez, D.: Evaluating fish scale
445 preservation in sediment records from the oxygen minimum zone off Peru, *Paleobiology*, 38(1),
446 52–78, doi:10.1666/10045.1, 2012.

447 Salvattecí, R., Field, D., Sifeddine, A., Ortlieb, L., Ferreira, V., Baumgartner, T., Caquineau, S.,
448 Velazco, F., Reyss, J. L., Sanchez-Cabeza, J. A. and Gutierrez, D.: Cross-stratigraphies from a
449 seismically active mud lens off Peru indicate horizontal extensions of laminae, missing sequences,
450 and a need for multiple cores for high resolution records, *Mar. Geol.*, 357, 72–89,
451 doi:10.1016/j.margeo.2014.07.008, 2014.

452 Salvattecí, R., Gutiérrez, D., Field, D., Sifeddine, A., Ortlieb, L., Bouloubassi, I., Boussafir, M.,
453 Boucher, H. and Cetin, F.: The response of the Peruvian Upwelling Ecosystem to centennial-scale
454 global change during the last two millennia, *Clim. Past*, 10(1), 1–17, doi:10.5194/cp-10-1-2014.

455 Saukel, C., Lamy, F., Stuut, J. B. W., Tiedemann, R. and Vogt, C.: Distribution and provenance
456 of wind-blown SE Pacific surface sediments, *Mar. Geol.*, 280(1-4), 130–142,
457 doi:10.1016/j.margeo.2010.12.006, 2011.

458 Scheidegger, K. F. and Krissek, L. A.: Dispersal and deposition of eolian and fluvial sediments
459 off Peru and northern Chile., *Geol. Soc. Am. Bull.*, 93(2), 150–162, doi:10.1130/0016-
460 7606(1982)93<150:DADDOEA>2.0.CO;2, 1982.

461 Sifeddine, A., Gutiérrez, D., Ortlieb, L., Boucher, H., Velazco, F., Field, D., Vargas, G.,
462 Boussafir, M., Salvattecí, R., Ferreira, V., García, M., Valdés, J., Caquineau, S., Mandeng Yogo,
463 M., Cetin, F., Solis, J., Soler, P. and Baumgartner, T.: Laminated sediments from the central
464 Peruvian continental slope: A 500 year record of upwelling system productivity, terrestrial runoff
465 and redox conditions, *Prog. Oceanogr.*, 79(2-4), 190–197, doi:10.1016/j.pocean.2008.10.024,
466 2008.

467 Smith, R. L.: Circulation patterns in upwelling regimes, *Coast. upwelling*, 13–35, 1983.

468 Stuut, J.-B. W., Kasten, S., Lamy, F. and Hebbeln, D.: Sources and modes of terrigenous sediment
469 input to the Chilean continental slope, *Quat. Int.*, 161(1), 67–76,
470 doi:10.1016/j.quaint.2006.10.041, 2007.

471 Stuut, J.-B. W., Prins, M. a., Schneider, R. R., Weltje, G. J., Jansen, J. H. F. and Postma, G.: A
472 300-kyr record of aridity and wind strength in southwestern Africa: inferences from grain-size
473 distributions of sediments on Walvis Ridge, SE Atlantic, *Mar. Geol.*, 180(1-4), 221–233,
474 doi:10.1016/S0025-3227(01)00215-8, 2002.

475 Suess, E., Kulm, L. D. and Killingley, J. S.: Coastal upwelling and a history of organic-rich
476 mudstone deposition off Peru, *Geol. Soc. London, Spec. Publ.*, 26(1), 181–197,
477 doi:10.1144/GSL.SP.1987.026.01.11, 1987.

478 Sun, D., Bloemendal, J., Rea, D. ., Vandenberghe, J., Jiang, F., An, Z. and Su, R.: Grain-size
479 distribution function of polymodal sediments in hydraulic and aeolian environments, and
480 numerical partitioning of the sedimentary components, *Sediment. Geol.*, 152(3-4), 263–277,
481 doi:10.1016/S0037-0738(02)00082-9, 2002.

482 Weltje, G. J. and Prins, M. a: Muddled or mixed? Inferring palaeoclimate from size distributions
483 of deep-sea clastics, *Sediment. Geol.*, 162(1-2), 39–62, doi:10.1016/S0037-0738(03)00235-5,
484 2003.

485

486

487

488

489

490 **RELEVANT CHANGES MADE IN THE MANUSCRIPT:**

491 It was rewritten part of the introduction with the aim to clarify the novelty and importance of this
492 publication for the knowledge of paleoclimate in the region. Moreover, was written a new chapter
493 called sedimentary settings to explain the favorable characteristics of the formation of laminated
494 sediments at Pisco region. This chapter explains also the mechanism of input of the lithological
495 terrigenous material over the continental shelf and the laminate formations.

496 In the same way it was added another chapter (Stacked record in Methods) to explain the principal
497 characteristics of the sediments cores (chronology, homogeneous deposits, slumps and
498 subsample) as well as the Method used for perform the record. Thus, new data was added as
499 supplementary data for explain this characteristics (supplementary material 1 and 2). It has been
500 enhanced the description of the grain size analysis in order to highlighting the use of lithological
501 total fraction. Finally, was rewritten part of the discussion and all the conclusions for better
502 explained the results and the contributions to the scientific progress of the paleoclimatology in
503 the Eastern Topical South Pacific during the last millennium.

504 **TERRIGENEOUS MATERIAL SUPPLY TO THE PERUVIAN CENTRAL**
505 **CONTINENTAL SHELF (PISCO 14°S) DURING THE LAST 14000 yr:**
506 **PALEOCLIMATIC IMPLICATIONS.**

507 F. Briceño-Zuluaga^{1,2}, A. Sifeddine^{1,2,3}, S. Caquineau^{2,3}, J. Cardich^{1,2}, R. Salvattecí^{2,3,5}, D.
508 Gutierrez^{2,4}, L. Ortlieb^{2,3}, F. Velazco^{2,4}, Hugues Boucher^{2,3}, Carine Machado^{1,2}.

509

510 ¹ Departamento de Geoquímica, Universidade Federal Fluminense - UFF, Niterói, RJ – Brasil.

511 ² LMI PALEOTRACES (IRD-France, UPMC-France, UA-Chile, UFF-Brazil, UPCH-Peru).

512 ³ IRD-Sorbonne Universités (UPMC, CNRS-MNHN), LOCEAN, IRD France-Nord, Bondy,
513 France.

514 ⁴ Instituto del Mar del Peru IMARPE.

515 ⁵ Institute of Geoscience, Department of Geology, Kiel University, Germany.

516

517 Correspondence to: franciscojavier@id.uff.br

518 **Abstract**

519 In the Eastern Pacific, lithogenic input to the ocean ~~is a~~ responds to variations of the atmospheric
520 and oceanic system variability and their teleconnections over different timescales. Atmospheric
521 (e.g., wind fields, precipitation), hydrological (e.g., fresh water plumes) and oceanic (e.g.,
522 currents) conditions determine the transport mode and the amount of lithogenic material
523 transported from the continent to the continental shelf. Here, we present the grain size distribution

524 of a composite record of two laminated sediment cores retrieved ~~in~~from the Peruvian continental
525 shelf, ~~covering that record~~ the last ~1400 yr at a sub-decadal to centennial time-series resolution.
526 We propose novel grain-size indicators of wind intensity and fluvial input that allow
527 reconstructing the oceanic-atmospheric variability modulated by sub-decadal to centennial
528 changes in climatic conditions. ~~We then discuss the paleo-environmental significance and the~~
529 ~~climatic mechanisms involved.~~ Four grain size modes were identified. Two are linked to aeolian
530 inputs (M3: 54.0 μm and M4: 91.0 μm on average), the third is interpreted as a marker of sediment
531 discharge (M2: 10 μm on average), and the last is without an associated origin (M1: ~3 μm). The
532 coarsest components (M3 and M4) dominated during the Medieval Climate Anomaly (MCA) and
533 the Current Warm Period (CWP) periods, suggesting that aeolian transport increased as
534 consequence of surface wind stress intensification. In contrast, M2 displays an opposite behavior,
535 exhibiting an increase in fluvial terrigenous input during the Little Ice Age (LIA), in response to
536 more humid conditions associated ~~to~~with El Niño like conditions. Comparison with other South
537 American paleoclimate records indicates that the observed changes are driven by interactions
538 between meridional displacement of the Intertropical ~~e~~Convergence ~~Z~~zone (ITCZ), ~~and of~~ the
539 South Pacific Sub-tropical High (SPSH) and Walker Circulation at decadal and centennial time
540 scales.

541 1. Introduction

542 ~~Along the Peruvian coast, the Pisco region represents a quite intense upwelling zone. This is due~~
543 ~~to intense alongshore wind, driving coastal upwelling and ultimately increasing marine~~
544 ~~productivity.~~ The Pisco region (~14-15°S) hosts one of the most intense coastal upwelling cells
545 off Peru due to the magnitude and persistence of alongshore equatorward winds during the annual
546 cycle (Fig. 1B). Regional wind can be affected at interannual timescales by El Niño Southern
547 Oscillation (ENSO) variability (i.e., enhanced or weakened during La Niña and El Niño events,
548 respectively), as well as by the Pacific Decadal Oscillation (PDO) at decadal timescales (Flores-
549 Aqueveque et al., 2015). ~~There are different sources and mechanisms controlling the~~ These factors
550 also affect the inputs of terrigenous material input to the Peruvian continental shelf. Saukel et al.
551 (2011) found that wind is the major transport agent of terrigenous material into the Peru–Chile
552 Trench, between 5°S and 25°S. Flores-Aqueveque et al. (2012) showed that in the arid region of
553 ~~n~~Northern Chile, transport of aeolian ~~coarser particles~~ (approximately ~100 μm) ~~transport~~ is
554 directly related to interannual variations in the domain of the strongest winds. The Pisco region
555 is also home to local dust storms called “Paracas”, which transport dust material to the continental
556 shelf as a response to seasonal erosion and transport events in the Ica desert (~15°S). This process
557 reflects atmospheric stability conditions and coastal sea surface temperature connections (Gay,
558 2005). In contrast, sediment fluvial discharge is more important in the ~~n~~Northern coast of Peru
559 where there are large rivers, and it decreases ~~decreasing~~ southward where arid conditions are

560 dominant (Garreaud and Falvey, 2009; Scheidegger and Krissek, 1982). This discharged material
561 is redistributed southward by coastal currents along the continental shelf (Montes et al., 2010;
562 Smith, 1983). In addition, small rivers exist in our study area, such as the Pisco ~~R~~river, which ~~has~~
563 ~~increased~~ flow during ~~strong—e~~El Niño events (Bekaddour et al., 2014). It has also been
564 demonstrated that during El Niño events and coincident positive PDO, there is an increase in
565 precipitation along ~~n~~Northern Peru and, consequently, higher river discharge, mainly from the big
566 rivers (e.g., the Santa ~~R~~river), whereas an opposite ~~behavior~~~~trend~~ is observed during La Niña
567 events and negative phase of PDO (Bekaddour et al., 2014; Böning and Brumsack, 2004; Lavado
568 Casimiro et al., 2012; Ortlieb, 2000; Rein, 2005, 2007; Scheidegger and Krissek, 1982; Sears,
569 1954).

570

571 Grain size distribution in marine sediments may indicate different sources and/or deposition
572 processes ~~that can be~~, expressed as polymodal distributions (e.g., Pichevin et al., 2005; Saukel et
573 al., 2011; Stuut et al., 2005, 2002; Sun et al., 2002; Weltje and Prins, 2003, 2007). ~~The~~~~is~~
574 polymodal distribution makes the classification of grain size composition an essential step in
575 ~~identifying the different sedimentary processes and the past environmental conditions behind~~
576 ~~them grain size classes for reconstructing past environmental conditions~~ (e.g., climate,
577 atmosphere and ocean circulation) (Alfaro et al., 2011; Bloemsa et al., 2012; Flores-Aqueveque
578 et al., 2012, 2015; Pichevin et al., 2005; Ratmeyer et al., 1999; Saukel et al., 2011; Stuut et al.,
579 2005, 2007; Sun et al., 2002). The grain-size distributions of lithogenic materials ~~o~~~~fin~~
580 sediments can thus be used to infer relative wind strengths and aridity on the assumption that
581 more vigorous atmospheric circulation will transport coarser particles to a ~~greater~~ ~~short~~ distance
582 and that the relative abundance of fluvial particles reflects ~~seasonal~~ precipitation patterns ~~excess~~
583 (e.g., Hesse and McTainsh, 1999; Parkin and Shackleton, 1973; Pichevin et al., 2005; Stuut and
584 Lamy, 2004; Stuut et al., 2002).

585 A significant number of ~~published papers~~ studies have described the climatic, hydrologic and
586 oceanographic changes during the last ~~2000~~ 1000 years ~~in~~~~on~~ the Peruvian continental shelf ~~in the~~
587 ~~Eastern Pacific region~~ (Sifeddine et al., 2008, Gutierrez et al., 2011, Salvattecí et al., 2014b, Ehlert
588 et al., 2015). ~~These climatic changes have affected the Humboldt Current circulation system and~~
589 ~~the precipitation pattern in the South Eastern Pacific in general, especially in the Pisco región~~
590 Evidences of changes in the Humboldt Current circulation system and in the precipitation pattern
591 have been reported. ~~in general, especially in the Pisco region. Agnihotri et al. (2008) suggested~~
592 ~~that the Peruvian Upwelling Ecosystem (PUE) is interspersed by periods of high and low~~
593 ~~productivity and denitrification, modulated by solar forcing at a centennial time scale. Salvattecí~~
594 ~~et al. (2014b) interpreted that~~ Salvattecí et al., (2014b) show that the ~~The~~ Medieval Climatic
595 Anomaly (MCA) exhibits two distinct patterns of Peruvian upwelling ~~PUE~~ characterized by

596 weak/intense marine productivity and sub-surface oxygenation, respectively, as a response to the
597 intensity to strength variation of SPSH linked to the Walker circulation. ~~Whereas during the Little~~
598 ~~Ice Age (LIA), an increased sediment discharge was driven by a southward displacement of the~~
599 ~~Intertropical Convergence Zone (ITCZ)~~ During the Little Ice Age (LIA), an increased sediment
600 discharge over the Pisco continental shelf was described, as well as a stronger oxygenation and
601 lower productivity (Sifeddine et al., 2008, Gutierrez et al., 2009). In addition, during the Current
602 Warm Period (CWP), the PUE exhibited 1) an intense Oxygen Minimum Zone (OMZ) and an
603 increase in marine productivity, 2) a significant SST cooling ($\sim 0.3\text{--}0.4^\circ\text{C decade}^{-1}$), and 3) an
604 increase in terrigenous material input (Gutierrez et al., 2011). ~~Those changes during the last~~
605 ~~Millennium in the South Eastern Pacific region seem to be linked to regional and local climatic~~
606 ~~phenomena, which had a significant impact on regional rainfall and local wind stress.~~
607 ~~Nevertheless, little is known about how the regional and local climatic variability impact~~
608 ~~sedimentation processes (i.e., Aeolian/Fluvial) in the Pisco region.~~

609 ~~this study aims to reconstruct the variation of the supply of terrigenous material to the Central~~
610 ~~Peruvian continental shelf, to determine how regional and local river fresh water discharge and~~
611 ~~local/regional wind field conditions have affected sedimentary deposition processes in the~~
612 ~~continental Peruvian shelf region (Pisco region), and to unravel the climatic mechanisms behind~~
613 ~~these processes during the last ~1100 yr.~~ Here we present new data regarding the effective mode
614 of transport of mineral fractions to the Pisco shelf during the last millennium, confirming previous
615 work, and bringing new highlights about the climatic mechanism behind Humboldt circulation
616 and atmospheric changes, especially during the MCA. Our results mark wind intensification
617 during second part of the MCA and CWP, in contrast to a decrease of the winds intensity during
618 the LIA and the first part of the MCA synchronous with fluvial discharge increase. Comparisons
619 with other paleoclimate records indicate that the ICTZ displacement, the SPSH and the Walker
620 circulation were the main drivers for the hydroclimate changes along the costal Peruvian shelf
621 during the last millennium.

622 2. Sedimentary settings.

623 Reinhardt et al., (2002); Suess et al., (1987) and Gutierrez et al., (2006) described the sedimentary
624 facies in the Peruvian shelf and the role of currents in the erosion process as well as the
625 redistribution and favorable hemipelagic sedimentation of material over the continental shelf.
626 These studies showed that high resolution sediment records are present in specific localities of
627 the Peruvian continental margin. Suess et al., (1987) described the two sedimentary characteristic
628 facies between $6 - 10^\circ\text{S}$ and between $11 - 16^\circ\text{S}$. The first one $6 - 10^\circ\text{S}$ (Salaverry Basin) is
629 characterized by no hemipelagic sediment accumulation because in this zone the southward
630 poleward undercurrent is strong. The second one, $11 - 16^\circ\text{S}$ Lima Basin, is characterized by a

631 lens shaped depositional center of organic-rich mud facies favored by oceanographic dynamics
632 from the position and low velocity of the southward poleward current on the continental shelf
633 (Reinhardt et al., 2002; Suess et al., 1987). High-resolution sediment echo sounder profiles further
634 characterize the mud lens nature and complement the continental shelf information (Salvatteci et
635 al., 2014a). These upper mud lenses are characterized by fine grain size, a diatomaceous,
636 hemiplegic mud with high organic carbon, and the absence of erosive and bioturbation process.

637 The Pisco continental shelf sediments are a composite of laminated sediments characterized by
638 an array of more or less dense sections of dark and light millimetric bands (Brodie and Kemp,
639 1994; Salvatteci et al., 2014a; Sifeddine et al., 2008). The laminae structure and composition
640 result from a complex interplay of factors including the terrigenous material input (both aeolian
641 and fluvial) the upwelling productivity and associated particle export to the seafloor (Brodie and
642 Kemp, 1994; Salvatteci et al., 2014a). The anoxic conditions favored by an intense OMZ
643 (Gutiérrez et al., 2006) and weak current activity at some areas (Reinhardt et al., 2002; Suess et
644 al., 1987) encourage the preservation of paleo-environmental signals and consequently, a
645 successful recording the climate variability.

646 Along the Peruvian coast lithogenic fluvial material is supplied by a series of rivers that are more
647 significant to the north of the study area (Lavado Casimiro et al., 2012; McPhillips et al., 2013;
648 Morera et al., 2011; Rein, 2005; Scheidegger and Krissek, 1982; Unkel et al., 2007). In fact,
649 Smith, (1983) concluded that sedimentary material can be transported for long distances in an
650 opposite direction of prevailing winds and surface currents in upwelling zones. In fact, the coastal
651 circulation off Peru is dominated by the poleward Peru-Chile undercurrent (PCUC), which flows
652 over the outer continental shelf and upper continental slope whereas the equatorward Peru coastal
653 current is limited to a few dozens of meters in the surface layer (Chaigneau et al., 2013). On the
654 other hand, several works have shown that precipitation, fluvial input discharge (Bekaddour et
655 al., 2014; Bendix et al., 2002; Lavado-Casimiro and Espinoza, 2014) and the PCUC increase
656 during the El Niño events (Hill et al., 1998; Strub et al., 1998; Suess et al., 1987). These
657 observations suggest a potential for the fluvial particles to spread over the continental margin
658 under wet paleoclimatic conditions (e.g., El Niño or El Niño-like). Lithogenic material in the
659 study area might also originate from wind-driven dust storms or “Vientos Paracas”, which are
660 more frequent and intense during Austral winters (Escobar Baccaro, 1993; Gay, 2005; Haney and
661 Grolier, 1991) and the saltation and suspension mechanisms with which this material reaches the
662 continental shelf.

663 **3. Materials and Methods**

664 **3.1. Stacked record.**

665 The B040506 “B6” (14° 07.90’ S, 76° 30.10’ W, 299 m water depth) and the G10-GC-01
666 “G10”(14° 22.96’ S, 076° 23.89’ W, 313 m water depth) sediment cores were retrieved from the
667 central Peruvian continental shelf in 2004 during the Paleo2 cruise onboard the Peruvian José
668 Olaya Balandra vessel (IMARPE) and in 2007 during the Galathea-3 cruise, respectively (Figure
669 1). We compared the age models and performed a laminae cross-correlation between the two
670 cores in order to develop a continuous record for the last millennium (Salvatteci et al., 2014a)
671 (Fig. 1S). The choice of these two cores was based on previous detailed stratigraphic investigations
672 and available complementary multi-proxy reconstructions (Gutiérrez et al., 2006, 2009; Salvatteci
673 et al., 2012, 2014a, 2014b; Sifeddine et al., 2008). The boxcore B06 (0.75 m length) is a laminated
674 core with a visible slump at ~52cm and 3 thick homogeneous deposits (1.5 to 5.0cm thick)
675 identified in the SCOPIX images. These intervals were not considered in our study (Fig. 1S). The
676 presence of filaments of the giant sulphur bacteria *Thioploca* spp in the top of core B06 confirms
677 the successful recovery of the sediment water interface.

678 According to the biogeochemical analysis in Gutierrez et al., (2009) (i.e., Palynofacies, Oxygen
679 Index (Rock-Eval), total organic carbon and $\delta^{13}\text{C}$) B06 is characterized by a distinctive shift at
680 ~30 cm. More details are provided by Sifeddine, et al. (2008), Gutiérrez et al. (2009) and
681 Salvatteci et al., (2014a). The age model of B6 was inferred from five ^{14}C -calibrated AMS age
682 distributions (Fig. 1S) and was shown that it covers the last ~700 yr. For the last century, which
683 is recorded only by B06, the age model was based on downcore natural excess ^{210}Pb and ^{137}Cs
684 distributions and supported by bomb-derived ^{241}Am distributions (Fig. 2S and Gutiérrez et al.,
685 (2009) The mass accumulation rate after ca. 1950AD was $0.036\pm 0.001 \text{ g cm}^{-2} \text{ y}^{-1}$ and before ca.
686 1820AD was $0.022\pm 0.001 \text{ g cm}^{-2} \text{ y}^{-1}$. On the other hand, the G10 is a gravity laminated sediment
687 core of 5.22 m presenting six units and exhibiting some minor slumping. The G10 age model was
688 based on thirty one samples of ^{14}C -calibrated AMS age distributions, showing that the core covers
689 the Holocene period (Salvatteci et al., 2014b, 2016). Here we used only a laminate section
690 between 18 and 51 cm that chronologically covered the MCA period (from ~900 to 1500) and
691 presented no slumps (Fig. 1S).

692 The spatial regularity of the initial core sampling combined with the naturally variable
693 sedimentation rate implied variable time rates between samples (150 samples in total). Each
694 sample is 0.5 cm thick in B6 and usually includes 1-2 laminae. On the other hand in core G10:
695 each sample is 1 cm thick including 3-4 laminae. The results considering the sedimentation rates
696 showed that the intervals during MCA, LIA and CWP span between 18, 7, and 3 years,
697 respectively. Because of differences in the subsampling thickness between cores and variable
698 sedimentation rates, results are binned by 20 year intervals (the lowest time resolution among
699 samples) after linear interpolation and 20-yr running mean of the original data set.

700 3.2. Grain size analyses

701 ~~To isolate the mineral fraction, organic material, calcium carbonates and biogenic silica were~~
702 ~~successively removed sample using H₂O₂ (30% at 50°C for 3 to 4 days), HCl (10% for 12 hours)~~
703 ~~and Na₂CO₃ (1 M at 90°C for 3 hours). Between each chemical treatment, samples were~~
704 ~~repeatedly washed with deionized water and centrifuged at 4000 rpm until the solution became~~
705 ~~neutral (pH: 6-7) again. Finally, all samples were passed through a 200 µm mesh before~~
706 ~~analysis because only particles having equivalent diameters less than 200 µm can be~~
707 ~~detected by the analytical method used. After pre-treatment, the grain size distribution was~~
708 ~~determined with an automated image analysis system (model FPIA3000, Malvern Instruments in~~
709 ~~which FPIA stands for Flow Particle Image Analyzer, ALYSES facilities at IRD, Bondy France).~~
710 ~~This system is based on a CCD (Charge Coupled Device) camera that captures images of all of~~
711 ~~the particles homogeneously suspended in a dispersal solution by rotation (600 rpm) in a~~
712 ~~measurement cell. After magnification (×10), the images are analyzed automatically and the~~
713 ~~equivalent spherical diameter (defined as the diameter of the spherical particle having the same~~
714 ~~surface as the measured particle) is determined. The optical magnification used (×10) implies that~~
715 ~~only particles with equivalent diameters between 0.5 and 200 µm are counted.~~

716 ~~It is worth noting that this system gives the size distribution and also displays images of the~~
717 ~~individual particles. If one ignores the images, this method provides size information comparable~~
718 ~~to that obtained with a laser granulometer. Nevertheless, the images are very useful to check the~~
719 ~~efficiency of the pre-treatments, and if necessary, non-mineral particles or aggregated mineral~~
720 ~~particles can be manually removed from the size distributions. The whole measurement range is~~
721 ~~divided into 225 equal logarithmical steps. Because the size bins selected by the manufacturer are~~
722 ~~quite narrow, the number of particles counted in some of them can be limited to just a few units,~~
723 ~~in which case the associated relative error can be very large. To reduce error, we decided to divide~~
724 ~~the number of size bins by a factor of 5 (we use 45 instead of the 225 original ones) and also to~~
725 ~~group the number of particles counted in each class. Grain size distributions are expressed as~~
726 ~~volume distributions.~~

727 To isolate the mineral terrigenous fraction, organic matter, calcium carbonate and biogenic silica
728 were successively removed from approximately 100 mg of bulk sediment sample using H₂O₂
729 (30% at 50°C for 3 to 4 days), HCl (10% for 12 hours) and Na₂CO₃ (1 M at 90°C for 3 hours)
730 respectively. Between each chemical treatment, samples were repeatedly rinsed with deionized
731 water and centrifuged at 4000 rpm until neutral pH. After pre-treatment, the grain size distribution
732 was determined with an automated image analysis system (model FPIA3000, Malvern
733 Instruments). This system is based on a CCD (Charge Coupled Device) camera that captures
734 images of all of the particles homogeneously suspended in a dispersal solution by rotation (600

735 rpm) in a measurement cell. After magnification ($\times 10$), particle images are digitally processed
736 and the equivalent spherical diameter (defined as the diameter of the spherical particle having the
737 same surface as the measured particle) is determined. The optical magnification used ($\times 10$) allows
738 the counting of particles with equivalent diameters between 0.5 and 200 μm . Prior to the FPIA
739 analysis, all samples were sieved with a 200- μm mesh in order to recover coarser particles. Since
740 particles $> 200 \mu\text{m}$ were never found in any samples, the grain size distribution obtained by the
741 FPIA method reliably represents the full particle size range in the sediment. A statistically
742 significant number of particles (hundreds of thousands up to 300.000) are automatically analysed
743 by FPIA providing particle size information comparable to that obtained with a laser
744 granulometer, along with images of the individual particles. Using the images to check the
745 efficiency of the pre-treatments, we ensured that both organic matter and biogenic silica had been
746 completely removed from all the samples. Finally, particle counting were binned into 45 different
747 size bins between 0.5 and 200 micron instead of the 225 set by the FPIA manufacturer in order to
748 reduce errors related to the presence of very few particles in some of the preselected narrow bins.
749 Grain size distributions are expressed as (%) volume distributions.

750 3.3. Determining sedimentary components and the deconvolution fitting model

751 As different ~~particles-sediment~~ transport/deposition processes are known to influence the grain-
752 size distribution of the lithic fraction of sediment material (e.g., Gomes et al., 1990; Holz et al.,
753 2007; Pichevin et al., 2005; Prins et al., 2007; Stuut et al., 2005, 2002; Sun et al., 2002; Weltje
754 and Prins, 2003, 2007; Weltje, 1997), identifying the individual components of the polymodal
755 grain size distribution is decisive for paleoenvironmental reconstructions. The numerical
756 characteristics [(e.g., amplitude (A), geometric mean diameter (G_{md}), and geometric standard
757 deviation (G_{sd})] of the individual grain size populations whose combination forms the overall
758 grain size distribution were determined for all samples using the iterative least-square method of
759 Gomes et al., (1990). This fitting method aims to minimize the square difference between the
760 measured volume-grain size distribution and the one computed from a -of particles counted in
761 each size class and that recomputed from the mathematical expression (based on log-normal
762 functions). The number of individual grain size populations to be used is determined by the
763 operator, and all statistical parameters (e.g., A , G_{md} and G_{sd}) are allowed to change from one
764 sample to another. ~~This presents a strong advantage compared to end-member modeling (e.g., of~~
765 ~~Weltje (1997)) in which the elementary distributions are maintained constant over the whole time~~
766 ~~series (the only changing parameter being their relative amplitude). Indeed, it is unlikely that the~~
767 ~~parameters that govern both transport and deposition of lithogenic sediments, and therefore grain~~
768 ~~size of particles, remain constant over time. This could lead to variations in statistical parameters~~
769 ~~(e.g., G_{md} and G_{sd}). This process presents a strong advantage compared to end-member~~
770 modeling (e.g., Weltje 1997) in which the individual grain size distributions are maintained

771 constant over the whole time series, the only fitting parameter being the relative amplitude, A.
772 Indeed, it is unlikely that the parameters that govern both transport and deposition of lithogenic
773 material, and therefore grain size of particles, remain constant over time. In turn, variations of
774 these parameters are expected to induce change of the grain size distribution parameters such as
775 Gmd and Gsd.

777 4. Results and discussion

778 4.1. Basis for interpretation

779 Both sediment cores (B06 and G10) exhibit roughly a bimodal grain-size distributions
780 representing significant variation in amplitude and width. These modes correspond to fine-grain-
781 size classes from ~3-15 μm and coarser grain size classes between ~50-120 μm (Fig. 3S). A
782 principal component analysis (PCA) based on the Wentworth (1922) grain-size classification
783 identifies four modes that could explain the total variance of the dataset (Fig. 4S). The measured
784 and modeled grain size distributions show high correlations ranging from $R^2=0.75$ to 0.90,
785 attesting that using 4 grain size modes is well adapted to our sediment samples and that thus the
786 computed ones may be modeled can provide reliable for further interpretations (Fig. 2A). Lower
787 correlations only occurred for 6 samples, all that are characterized by small proportions of
788 terrigenous material compared to biogenic silica, organic matter and carbonates. Lower
789 correlations only occurred when the proportion of lithological material proportion was small
790 compared to silica, organic matter and bulk carbonate (6 samples). In these cases, This situation
791 was is met when the number of lithicological particles remaining after the chemical attack was
792 small, which increased the associated relative error, of these samples was significantly lower,
793 placing it at the limit of statistical representation. However, these samples have been included in
794 the data set since because they all presented a high contribution of coarser particles.

795 Grain size parameters are presented in Table 1. The first mode (M1), with a Gmd of approximately
796 $3 \pm 1 \mu\text{m}$, and the second one (M2), with a Gmd of $10 \pm 2 \mu\text{m}$, are characterized by large Gsd
797 ($\sim 2\sigma$), indicating a low degree of sorting. Such low degree of sorting suggests a slow and
798 continuous depositional process as occurs in other environments (Sun et al., 2002). The coarsest
799 modes M3 and M4 display mean Gmd values of $54 \pm 12 \mu\text{m}$ and $91 \pm 13 \mu\text{m}$, respectively. These
800 modes present Gsd values close to 1σ . The Gmd values of the two coarsest modes are consistent
801 with the optimal grain size transported under conditions favorable to soil (lack of vegetation, low
802 threshold friction velocity, surface roughness and low soil moisture) and low wind friction
803 velocity (Iversen and White, 1982; Kok et al., 2012; Marticorena and Bergametti, 1995;
804 Marticorena, 2014; Shao and Lu, 2000). Such conditions prevail in the studied area because the

805 central coastal Peru consists of a sandy desert area characterized by no rain, a lack of vegetation
806 and persistent wind (Gay, 2005; Haney and Grolier, 1991).

~~807 Geometrical standard deviation (Gsd) vs. Geometrical mean diameter (Gmd) (Fig. 2B). The first
808 mode (M1), with a Gmd of approximately $3 \pm 1 \mu\text{m}$, and the second one (M2), with a Gmd of 10
809 $\pm 2 \mu\text{m}$, are characterized by larger Gsd, indicating a low degree of sorting. According to Sun et
810 al. (2002), such a low degree of sorting (Gsd $> 2\sigma$) suggests a slow and continuous depositional
811 process (Sun et al., 2002). The coarsest modes M3 and M4 display mean Gmd values of 54 ± 11
812 μm and $91 \pm 11 \mu\text{m}$, respectively. These modes presented Gsd values close to 1σ . This is
813 consistent with the optimal grain size transported under favorable erosional soil properties and
814 low wind friction velocity (Iversen and White, 1982; Shao and Lu, 2000; Marticorena, 2014).~~

815 In the vicinity of desert areas, where wind-blown transport prevails, particles with grain size as
816 high as $\sim 100 \mu\text{m}$ can accumulate in marine sediments (e.g., Stuut et al., 2007; Flores-Aqueveque
817 et al., 2015) or even in lacustrine sediments (An et al., 2012). Indeed, Stuut et al., (2007) reported
818 the presence of distributions typical of wind-blown particles with $\sim 80 \mu\text{m}$ grain size ($\sim 29^\circ\text{S}$ North
819 Chile) that is consistent with our results. In the studied area, the emission and the transport of
820 mineral particles are related to the strong wind events called “Paracas”. Paracas dust emission is
821 a local seasonal phenomenon that preferentially occurs in winter (July-September) and is due to
822 an intensification of the local surface winds (Escobar Baccaro, 1993; Haney and Grolier, 1991;
823 Schweigger, 1984). The pressure gradient of sea level between $15^\circ\text{--}20^\circ\text{S}$, 75°W is the controlling
824 factor of Paracas winds (Quijano, 2013), along with local topography (Gay, 2005). Coarse
825 particles found in continental sediments off Pisco cannot have a fluvial origin because substantial
826 hydrodynamic energy is necessary to mobilize particles of this size ($50\text{--}100 \mu\text{m}$), and this region
827 is devoid of large rivers (Reinhardt et al., 2002; Scheidegger and Krissek, 1982; Suess et al.,
828 1987).

~~829 These coarse particles cannot have a fluvial origin because substantial hydrodynamic energy is
830 necessary to mobilize particles of this size, and because this region is devoid of large-
831 sized rivers (Scheidegger and Krissek, 1982). Rein et al., (2004), followed by Bekaddour
832 et al. (2014), discussed the influence of the changes in the climatic regime as a control
833 of the intensification and variability in the sedimentation of detrital material of fluvial
834 origin in the region. Thus, the continental shelf off of Pisco receives coarse aeolian particles by
835 saltation and suspension processes linked to Paracas events as well as fluvial particles from the
836 few rivers that reach the coast in this region.~~

837 Therefore, the coarsest modes (M3 and M4) can be interpreted as markers of aeolian transport
838 resulting from surface winds and emission processes (e.g. ~~Paracas events~~) (Flores-Aqueveque et
839 al., 2015; Hesse and McTainsh, 1999; Marticorena and Bergametti, 1995; McTainsh et al., 1997;

840 Sun et al., 2002) and ~~These two components (M3 and M4)~~ indicate a local and proximal source
841 to aeolian material (i.e., Paracas winds). This interpretation is in contrast to the Atacama Desert
842 source suggested by Ehlert et al., (2015) and Molina-Cruz, (1977). Ehlert et al. (2015), who used
843 the same sediment core (B06), and also indicated difficulties in the interpretation of the detrital
844 Sr isotopic signatures as an indicator of the sources. These difficulties can be associated with the
845 variability of the $^{87}\text{Sr}/^{86}\text{Sr}$ due to grain size (Meyer et al., 2011). The finest M1 component (~ 3
846 μm) may be linked to both aeolian and fluvial transport mechanisms, or alternatively, may come
847 from aggregates of other particles. Thus, because its origin is difficult to determine, and because
848 its trend appears as relatively independent from the other components, we do not further use it.

~~849 The M2 component ($\sim 10 \mu\text{m}$) is interpreted as characteristic of fluvial transport (Koopmann,
850 1981; McCave et al., 1995; Stuut et al., 2007). The fluvial origin of the M2 component is also
851 supported by its trend along the core, which differs from those of M3 and M4 from aeolian origin.
852 A fluvial origin of this M2 component is also supported by geochemical proxies, by an increase
853 in the Ti content input (Sifeddine et al., 2008 and Salvattecchi et al., 2014b) and radiogenic isotope
854 compositions of detrital components (Ehlert et al., 2015), indicating more terrigenous transport
855 during the LIA, where humid conditions are dominant. This M2 component is interpreted as
856 linked to river material discharge, mostly from the north Peruvian coast, and redistributed by
857 oceanic southward coastal currents (Montes et al., 2010; Rein et al., 2004; Scheidegger and
858 Krissek, 1982; Unkel et al., 2007).~~

859 The M2 component ($\sim 10 \mu\text{m}$) is interpreted as an indicator of fluvial transport (Koopmann, 1981;
860 McCave et al., 1995; Stuut and Lamy, 2004; Stuut et al., 2002, 2007). Indeed, this is consistent
861 with the reported by Stuut et al., (2007) for the fluvial mud ($\sim 8\mu\text{m}$) in the South of Chile ($>37^\circ\text{S}$)
862 where the terrigenous input is dominated by fluvial origins. A fluvial origin of this M2 component
863 is also supported by showing the same trend in the geochemical proxies, such as radiogenic
864 isotope compositions of detrital components (Ehlert et al., 2015), mineral fluxes (Sifeddine et al.,
865 2008) or %Ti (Salvattecchi et al., 2014b), indicating more terrigenous transport during the LIA,
866 when humid conditions were dominant. The M2 component is interpreted as being linked to river
867 material discharge, mostly from the north Peruvian coast, and redistribution by the PCUC and
868 bottom currents (Montes et al., 2010; Rein et al., 2004; Scheidegger and Krissek, 1982; Unkel et
869 al., 2007).

870 4.2. Fluvial and aeolian input variability during the past ~ 1000 yr

871 Grain size component (M2, M3 and M4; Table 1) variations in along the composite records (B06
872 and G10) express changes in wind stress and fluvial runoff ~~at and wind stress~~ multi-decadal to
873 centennial-scale changes during the last millennium. ~~This variability allows ed the identification~~
874 ~~of three major climate periods: MCA, LIA and CWP in the last millennium~~. The sediments

875 deposited during the MCA exhibit two contrasting patterns of grain size distributions. In the first
876 sequence, dated from 900 to 1170 AD, low values of D_{50} were found varying around $16 \pm 6 \mu\text{m}$,
877 and explained by $50 \pm 10\%$ M2, $18 \pm 7\%$ M3, $21 \pm 8\%$ M4 and $11 \pm 4\%$ M1 contributions. A second
878 sequence, dated from 1170 to 1450 AD, was marked by high values of D_{50} in the range of 28 ± 17
879 μm , with average contributions of $14 \pm 6\%$ for M1 and $41 \pm 10\%$ for M2, and values around $21 \pm$
880 9% for M3 and $24 \pm 15\%$ for M4. These results indicate high variability of transport particles
881 during the MCA, with more fluvial sediment discharge from 900 to 1170, and increase of aeolian
882 material input between 1170 and 1450 AD that suggest a last period of enhancement in the surface
883 wind stress (Fig. 3A). during the MCA exhibit two contrasting patterns of grain size distributions.
884 A first sequence, dated from 1050 to 1170 AD has, low values of D_{50} that vary around $16 \pm 6 \mu\text{m}$,
885 and are explained by $50 \pm 14\%$ M2, $16 \pm 8\%$ M3, $21 \pm 5\%$ M4 and $13 \pm 5\%$ M1 contributions. A
886 second sequence, dated from 1170 to 1450 AD, was marked by high values of D_{50} in the range
887 of $34 \pm 18 \mu\text{m}$, with average contributions of $36 \pm 8\%$ for M2, $21 \pm 10\%$ for M3, $29 \pm 15\%$ for M4
888 and $14 \pm 6\%$ for M1. These results indicate high variability of transport of particles during the
889 MCA, with more fluvial sediment discharge from 1050 to 1170, followed by an aeolian transport
890 increase between 1170 and 1450 AD (Fig. 3).

891

892 During the LIA (1450 – 1800 AD), the deposited particles were dominated by fine grain sizes
893 with a D_{50} varying around an average of $15 \mu\text{m}$, explained by $53 \pm 15\%$ M2 contribution. In
894 contrast, the contributions of The M3 presented an average contribution of $19 \pm 9\%$ and ranged
895 from 4 to 45%, whereas M4 showed an average contribution of $14 \pm 11\%$ and varied from 0 to
896 44% during the same period. This significant The dominant contribution of the finest-sized
897 particles of M2 suggests a high fluvial terrigenous input to the Peruvian continental shelf. It is
898 important to note that M2 contributions increased from the beginning to the end of the LIA at
899 ~ 1800 AD (Fig. 3A), suggesting a gradual increase in fluvial sediment discharge input relate to
900 enhancement of the continental precipitation (Fig. 3C). Indeed, during the LIA, our results agree
901 with previous studies interpretations of wet conditions along the Peruvian coast (Apaéstegui et al.,
902 2014a; Gutiérrez et al., 2008; Salvattecchi et al., 2014b; Sifeddine et al., 2008), indicating wet
903 conditions over the drainage basins. These results also imply that this period was characterized
904 by weak surface winds, and hence a weaker coastal upwelling.

905 Finally, D_{50} variations show high variability during the last 250 yr of these two periods (1750 to
906 1850 AD and 1900 to 1960 AD within the CWP) characterized by high D_{50} values around 45
907 μm , with $\sim 40\%$ and $\sim 30\%$ M4 and M3, respectively. From 1850 to 1900 AD and from 1960 to
908 2000 AD in the CWP, D_{50} displayed values of approximately $20 \mu\text{m}$ explained by $\sim 40\%$ M2.
909 Our results indicate a clear increase in coarse (M3 and M4) aeolian material deposition during the

910 ~~CWP, especially from 1750 to 1850 AD and 1900 to 1960 AD. Moreover, it is noteworthy that~~
911 ~~during these two periods, coarser particles as large as ~120 μm (in M4 component) were found,~~
912 ~~indicating extreme wind stress events (Fig. 3F). On the contrary, the fluvial sediment discharge~~
913 ~~was the dominant transport mechanism between 1850 and 1900 AD, as well as between 1960 and~~
914 ~~2000 AD. The finest particles exhibit a progressive increase during the last 50 years, suggesting~~
915 ~~an increase of the terrigenous sediment input from rivers discharge. A similar trend was observed~~
916 ~~in the total terrigenous flux record of Pisco and Callao (Sifeddine et al., 2008).~~

917 Subsequently, *D*50 variations show multidecadal variability during the last ~200 yr that is divided
918 into three distinctive periods. The first one from ~1800 to 1850 AD shows dominance of coarse
919 particles around 50 μm, explained by the high contribution of M3 and M4 (up to 45% and 50%
920 respectively) during this period. These results suggest a period of drier climate and very strong
921 wind conditions. The second one from 1850 to 1900AD displays values around ~20 μm explained
922 by ~40% of M2, ~20% of M3 and ~20% of M4 that suggests that fluvial sediment discharge was
923 the dominant transport mechanism, although not as significant as during the LIA. The third period
924 spans from 1900 AD to the final part of record and covers the CWP. Our results reveal a
925 dominance of coarse particles during the most of this period (*D*50 up to of 80 μm) that arise from
926 high contributions of M3 and M4 (~40% and ~50% respectively). However a clear decrease of
927 the *D*50 is displayed at the end of this period that is explained by a decrease of contributions of
928 the aeolian component M4 (~20%), although the contribution of M3 and M2 remain relatively
929 stable (~25% and 30% respectively). These conditions display no clear dominance of a given
930 transport mode during this time. In addition, markedly coarser particles (in M4 component) were
931 very common during this time (the last 200yr) indicating a strong probability of extreme wind
932 stress events (Fig. 3F).

933 4.3. Climatic interpretations

934 Our findings suggest a combination ~~betweenof~~ regional and local atmospheric circulation
935 mechanism changes, ~~thatwhich~~ controlled the pattern of sedimentation in the study region. Our
936 record is located under the contemporary seasonal Paracas dust storm path, but it also records
937 discharged fluvial muds, ~~that ar, often~~ supplied by the rivers along the Peruvian coast. Hence, this
938 record is particularly well suited for a reconstruction of continental runoff/wind intensity in the
939 central Peruvian continental shelf during the last millennium. The interpretation of the changes in
940 the single records of the components (M2, M3 and M4) and their associations (e.g., ratios) can
941 reflect paleoclimatic variations in response to changes in atmospheric conditions. Here, we used
942 the ratio between the aeolian components, defined as the contribution of the stronger winds over
943 total wind variability: $M4/(M3+M4)$. We ~~considerused~~ this ratio as a proxy of the local wind
944 surface intensity and thus as of the SPSH atmospheric circulation (Fig. 4F). Previous studies have

945 ~~similarly and successfully~~ In fact, the use of grain-size fraction ratios as a paleoclimate indicator
946 for proxies of atmospheric conditions and circulation has been successfully applied to explain
947 ~~different other sediment~~ records (Holz et al., 2007; Huang et al., 2011; Prins, 1999; Shao et al.,
948 2011; Stuut et al., 2002; Sun et al., 2002; Weltje and Prins, 2003).

949 ~~As explained above, the MCA was characterized by a sinuous peak structure that depicts two~~
950 ~~different climate stages. A first stage spanning from ~900 to 1170 A.D. is dominated by a high~~
951 ~~sediment fluvial discharge linked to a precipitation increase (Fig. 4E). This precipitation increase~~
952 ~~can be explained by the Southward displacement of the ITCZ (Fig. 4B) and a reduction of the~~
953 ~~SPSH circulation strong (weaker favorable upwelling winds or surface winds intensity) (Fig. 4F).~~
954 ~~This pattern linked to the reorganization of the atmospheric and ocean circulation, that is also~~
955 ~~underlined by Salvattei et al. (2014b) using biogeochemical proxies from an ocean sediment~~
956 ~~record, showing sub-oxic sediment conditions (demonstrated by high values of the Re/Mo ratio),~~
957 ~~indicating a weaker OMZ intensity (Fig. 4C) probably associated with El Niño-like conditions.~~
958 ~~Less fluvial input (i.e., dry continental conditions) and more intense surface winds characterized~~
959 ~~the second stage of the MCA (~1170 A.D. to 1350 A.D.) linked to the intensification of SPSH as~~
960 ~~a response of a northward ITCZ-SPSH meridional displacement and more la Niña-like conditions.~~
961 ~~In fact, the wind intensity trend during this period is consistent with the warmer temperature~~
962 ~~recorder at the west of Pacific during the last millennium (Fig. 4A). These latter features are in~~
963 ~~phase also with a period of strong OMZ off of Pisco (Fig. 4C), associated with more intense~~
964 ~~upwelling conditions from a more intense Walker circulation. In agreement with Salvattei et al.~~
965 ~~(2014b), these patterns are consistent with persistent austral summer-like conditions.~~

966 As explained above, the MCA was characterized by a sine-like peak structure that depicts two
967 different climate stages. During the first stage spanning from ~1050 to 1170 AD the fluvial input
968 show a peak centered at 1120 AD linked to a precipitation increase accompanied by a decrease in
969 wind intensity. Those results suggest a southward ITCZ displacement (Fig. 4E) as a response to
970 more El Niño like conditions as suggested by Rustic et al., (2015) (Fig 4 G and H). In contrast,
971 during the second stage the surface winds had their greatest intensity with a peak centered at
972 ~1200 AD as a consequence of displacement of the ITCZ-SPSH system. The displacement of the
973 SPSH core towards eastern South American coast intensified alongshore winds as a regional
974 response to stronger Walker circulation. These features are in agreement with the ocean
975 thermostat mechanism proposed by Clement et al., (1996). This mechanism produces a shallow
976 thermocline in the eastern Pacific (Fig. 4G and H) and consequently more intense upwelling
977 conditions and a stronger OMZ offshore of Pisco recorded in low values of the Re/Mo ratio (Fig.
978 4D). These two patterns (i.e., enhanced fluvial transport/enhanced wind intensity) might have
979 been triggered by the expression of Pacific variability at multidecadal timescales with the
980 combined action of the Atlantic Multidecadal Oscillation (AMO). Indeed other works provide

981 evidence during the MCA for low South American Monsoon System (SAMS) activity at
982 multidecadal timescales driven by the AMO (Fig. 4F) (Apaéstegui et al., 2014; Bird et al., 2011;
983 Reuter et al., 2009). Thus, besides the displacement of the ITCZ', the AMO could have modulated
984 Walker circulation at a multidecadal variability during the MCA through mechanisms such as
985 those described by Mcgregor et al., (2014) and Timmermann et al., (2007).

986 Our results combined with other paleo-reconstructions suggest that the LIA ~~exhibited was~~
987 ~~accompanied by~~ a weakening of the regional atmospheric circulation ~~and of the and winds~~
988 ~~favorable for~~ upwelling- ~~favorable winds~~. During the LIA, the mean climate state was controlled
989 by a gradual intensification of the fluvial input ~~of sediments~~ to the continental shelf, thus
990 indicating ~~more wetter~~, El Niño-like conditions ~~consistent with the El Niño-like conditions~~ (Fig.
991 4E). These ~~features conditions~~ are confirmed by an increase ~~of in~~ the terrigenous sediment flux,
992 as described by Sifeddine et al. (2008) and Gutierrez et al., 2009 (Fig 4D) and ~~demonstrated~~ by
993 ~~changes of~~ the radiogenic isotopic composition of the terrigenous fraction (Ehlert et al., 2015).
994 ~~These This increase in~~ wet conditions ~~is are~~ also marked by an intensification of the South
995 American Monsoon System (SAMS) ~~and the southern meridional displacement of the ITCZ, as~~
996 ~~evidence by.~~ Paleo-precipitation records ~~in the Andes and in the Cariaco Trench support these~~
997 ~~regional characteristics~~ (Apaéstegui et al., 2014a; Haug et al., 2001; Peterson and Haug, 2006).
998 ~~These conditions were consistent and suggest a direct relationship with the southern meridional~~
999 ~~displacement of the ITCZ (Fig. 4B).~~ ~~At the same time, a~~ ~~This feature is followed accompanied by~~
1000 ~~the~~ prevalence of weak surface winds (Fig. 4A) ~~F~~ and ~~an increase of subsurface oxygenation~~
1001 ~~driving noticeable~~ sub-oxic conditions in the ~~sea~~ surface sediment ~~are recorded~~ (Fig. 4D) ~~C~~. These
1002 characteristics also support the hypothesis of the ITCZ-SPSH southern meridional displacement
1003 and are consistent with a weakening of the Walker circulation (Fig. 4G) ~~A~~.

1004 The transition period between the LIA and CWP appears as an abrupt event showing a progressive
1005 positive anomaly in the wind intensity ~~synchronous with a and a strong and~~ rapid decrease in the
1006 fluvial input to the continental shelf (Fig. 4A) ~~F~~ and ~~BE~~). This ~~transitions suggests suggest~~ a rapid
1007 change of ~~meridional the combination of a meridional~~ (ITCZ-SPSH) and ~~a zonal the~~ (Walker)
1008 circulation ~~interconnection(ENSO) factors (Fig. 4A and B)~~, which controls the input of
1009 terrigenous material (Fluvial/Aeolian). ~~Gutiérrez et al.(2009) found evidence of a large The~~
1010 ~~results suggest that precipitation pattern is affected more rapid and suddenly in comparison with~~
1011 ~~the surface wind intensity. Gutiérrez et al.(2009) found evidence of a large~~ reorganization in the
1012 tropical Pacific climate with immediate effects on ocean biogeochemical cycling and ecosystem
1013 structure at the transition between the LIA and CWP. ~~The increase in the wind intensity~~ (Fig. 4F)
1014 ~~suggests northward displacement of the ITCZ-SPSH system, which in turn~~ The increases ~~in the~~
1015 regional winds ~~circulation (favoring aeolian erosive processes) and~~ simultaneously leads to an
1016 increase in the OMZ intensity related to upwelling intensification (Fig 4C).

1017 Finally, during the CWP (~1900 A.D. to present), ~~negative anomalies in the~~ trend to seadying of
1018 of low fluvial input (Fig. 4EB) ~~were~~ as combined with an increase in wind intensity (Fig. 4FA)
1019 that was coupled to a strong OMZ. This setting suggests the northernmost ITCZ-SPSH system
1020 position ~~This setting suggests stronger modification in the atmospheric regime of terrigenous~~
1021 fluvial input when the ITCZ-SPSH system is at its northernmost position (Fig. 4E and F). This
1022 hypothesis is supported by other studies on the continental shelf of Peru (Salvatteci et al., 2014b)
1023 and also in the Eastern Andes where a decrease in rainfall of between ~10 – 20% relative to the
1024 LIA was reported for the last century (Reuter et al., 2009) ~~This hypothesis is supported by other~~
1025 ~~studies on the continental shelf of Peru (Salvatteci et al., 2014b) and also in the Eastern Andes~~
1026 ~~where an increase in rainfall (between ~10 – 20%) was detected during the LIA, with respect to~~
1027 ~~the subsequent 200 years (Reuter et al., 2009).~~ Enhancement of wind intensity is also consistent
1028 with the multidecadal coastal cooling and increase of ~~This trend is consistent with the increase in~~
1029 upwelling productivity since the late nineteenth century (Gutiérrez et al., 2011; Salvatteci et al.,
1030 2014b; Sifeddine et al., 2008) and confirms the relationship between the intensification of the
1031 upwelling activity induced by the variability of the regional winds intensity from SPSH
1032 displacement ~~and circulation.~~

1033 The increase in the wind intensity over the past two centuries likely represents ~~the~~ result of the
1034 modern positioning of the ITCZ – SPSH system and the associated intensification of the local and
1035 regional winds (Fig. 4F). The contributions of ~~Nevertheless, the~~ aeolian deposition material (Fig.
1036 3E and F) and in consequence the wind intensity and its variability during the last 100 yr are
1037 stronger than during the second sequence of the MCA (Fig. 4AF) under similar conditions (i.e.,
1038 position of the ITCZ-SPSH system, Fig. 4B). This variability suggests ~~implies~~ an additional
1039 forcing mechanism in additions to the enhancement of the winds intensity, one that may be related
1040 to the currents climate change conditions ~~This trend suggests an additional forcing in the~~
1041 ~~intensification of the atmospheric circulation consistent with the pattern of climate change (~~
1042 Bakun, 1990; England et al., 2014; Sydeman et al., 2014). ~~Finally, the decrease in runoff in the~~
1043 ~~same period displayed by the M2 component reflects a tendency for drier regional conditions in~~
1044 ~~comparison with the LIA period (Fig. 4E).~~ ~~However~~ Moreover, during the CWP, the wind
1045 intensity intensification showed a direct ~~close~~ relationship with the OMZ strength variability (Fig.
1046 4AC and FD), ~~reinforcing the interpretation of wind intensification consequence of a~~
1047 ~~strengthening of the SPSH.~~ that suggest an increase in the zonal gradient and thus in the Walker
1048 circulation on a multidecadal scale.

1049 Our record shows that on a centennial scale, the fluvial input changes are driven by the meridional
1050 ITCZ position and a weak gradient of the Walker circulation, consistent with El Niño like
1051 conditions. In contrast, variations of the surface wind intensity are linked to the position of the
1052 SPSH modulated by both the meridional variation of the ITCZ and the intensification of the zonal

1053 gradient temperature related with the Walker circulation and expressing La Niña like conditions.
1054 A clear relation between the zonal circulation and wind intensity at a centennial time scale is
1055 displayed. All these features modulate the biogeochemical behavior of the Peruvian upwelling
1056 system.

1057
1058 ~~Variations of the fluvial input exhibited a centennial pattern variability along the last millennium,~~
1059 ~~showing an intense activity fluvial input during the first period of the MCA and during the LIA.~~
1060 ~~Thus, a mean climate state period of wet conditions and reduced wind intensity in this time is~~
1061 ~~indicated (Fig. 4E). In contrast, the second period of MCA and CWP exhibits little fluvial input~~
1062 ~~and more vigorous wind intensity, being that the last one exhibited more the latter with larger~~
1063 ~~positive anomalies. This variability suggests an additional mechanism to the enhancement of the~~
1064 ~~winds intensity maybe relate to the climate change conditions. The inverse relationship A good~~
1065 ~~match between the Ti content record from terrigenous input to the Cariaco basin (Fig. 4B) and~~
1066 ~~the decadal and centennial variation in the fluvial input in to the Peruvian continental shelf~~
1067 ~~supports the hypothesis that both systems are controlled by a common climatic mechanism, , e.g.,~~
1068 ~~This condition is related to the meridional ITCZ displacement as described by Haug et al., (2001),~~
1069 ~~Hyeong et al., (2006), Peterson and Haug, (2006) and most recently by Sachs et al., (2009).~~
1070 ~~Consequently, a southward/northward ITCZ displacement and is related with a~~
1071 ~~weakening/enhancement of the SPSH system off Central and Southern Peru over the East Pacific~~
1072 ~~would be expected. These conditions will contribute to the weakening or strengthening of the~~
1073 ~~surface winds on multidecadal time scale. In turn, these conditions modulate the biogeochemical~~
1074 ~~behavior of the Peruvian upwelling system. On the other hand, a clear relationship between the~~
1075 ~~zonal circulation and wind intensity at centennial time scale is display. During the second part of~~
1076 ~~the MCA and during CWP La Niña like conditions prevail at the same time strongest wind are~~
1077 ~~exhibited these conditions might strong circulation under these features.~~

1078 **5. Conclusions**

1079 ~~Four types of terrigenous components (M2, M3 and M4) related to different transport modes in~~
1080 ~~the continental shelf along the last millennium were identified in a sediment record. The M2~~
1081 ~~mode is an indicator of hemipelagic fluvial input; meanwhile, the M3 and M4 components are~~
1082 ~~related to aeolian transport. A vigorous transport of aeolian and fluvial components exhibits~~
1083 ~~centennial variability and shows a relationship with atmospheric conditions. The MCA and~~
1084 ~~CWP periods showed an increment in the wind intensity, whereas the LIA was characterized by~~
1085 ~~intense fluvial input. Comparison between records reveals a coherent match between the~~
1086 ~~meridional displacement of the ITCZ SPSH system and the regional fluvial and aeolian~~
1087 ~~terrigenous input variability. The aeolian input intensity and the anoxic conditions recorded by~~

1088 ~~marine sediments showed a close link that suggests a mechanism associated with SPSH~~
1089 ~~displacement. Changes in sediment discharge to the continental shelf are linked to the~~
1090 ~~southward displacement of the ITCZ-SPSH. A progressive intensification of the wind intensity~~
1091 ~~recorded during the CWP can be related to the strength of the Walker circulation, favoring La~~
1092 ~~Niña events, which allow for an increase in regional wind intensity and consequently~~
1093 ~~OMZ intensification. Based on this trend, our record shows high decadal variability of~~
1094 ~~terrigenous versus aeolian transport.~~

1095 Study of the grain size distribution in laminated sediments from the Pisco Peruvian shelf has
1096 allowed the reconstruction of changes in wind intensity and terrigenous fluvial input at centennial
1097 and multidecadal time scales during the last millennium. The long-term variation of M2 (~10 μ m)
1098 mode is an indicator of hemipelagic fluvial input related to the regional precipitation variability.
1099 Meanwhile, the M3 (54 \pm 11 μ m) and M4 (91 \pm 11 μ m) components are related to aeolian transport
1100 and thus with both local and regional wind intensity. The temporal variations of these fractions
1101 indicate that the MCA and CWP periods were characterized by an increment in the coarse particle
1102 transport (M3 and M4) and thus an enhancement of the surface wind intensity, whereas the LIA
1103 was characterized by stronger fluvial input as evidence from an increase of fine (M2) particles.
1104 Comparison between records reveals a coherent match between the meridional displacement of
1105 the ITCZ-SPSH system and the regional fluvial and aeolian terrigenous input variability. The
1106 ITCZ-SPSH system northern displacement during the second period of the MCA and the CWP
1107 was associated with the intensification of the Walker cell and La Niña Like conditions, resulting
1108 in stronger winds, upwelling-favorable conditions, enhanced marine productivity and greater
1109 oxygen depletion in the water column. In contrast, the southward migrations of the ITCZ-SPSH
1110 system during the LIA correspond to an enhancement to the South American Monsoon circulation
1111 and El Niño like conditions, driving the increase in the precipitation and the terrigenous fluvial
1112 input to the Pisco continental shelf, lower productivity and increased oxygenation. Two patterns
1113 observed during the MCA, respectively marked by fluvial intensification and wind intensification,
1114 could have been forced by Pacific Ocean variability at multidecadal timescales. Further studies
1115 of the paleo-wind reconstruction at high time-resolution, combined with model simulation, are
1116 needed to better understand the interplay between the Pacific and Atlantic Ocean connection on
1117 climate variability as evidenced by McGregor et al., (2014) in the modern Pacific climate pattern.

1118 **6. Acknowledgements**

1119 This work was supported by the International Joint Laboratory "PALEOTRACES" (IRD-France,
1120 UPMC-France, UFF-Brazil, UA-Chile, UPCH-Peru), the Department of Geochemistry of the
1121 Universidade Federal Fluminense-UFF (Brazil), the ALYSES analytical platform (IRD/UPMC),
1122 the Peruvian Marine Research Institute (IMARPE) and the Geophysical Peruvian Institute (IGP).

1123 It was also supported by the collaborative project Chaire Croisée PROSUR (IRD). We deeply
1124 thank the CAPES-Brazil for the scholarship. We are also grateful to the anonymous reviewers for
1125 their constructive and helpful suggestions to improve this manuscript.

1126 3 7. Bibliography

1127 Agnihotri, R., Altabet, M. a., Herbert, T. D. and Tierney, J. E.: Subdecadally resolved
1128 paleoceanography of the Peru margin during the last two millennia, *Geochemistry Geophys.*
1129 *Geosystems*, 9(5), Q05013, doi:10.1029/2007GC001744, 2008.

1130 Alfaro, S. C., Flores-Aqueveque, V., Foret, G., Caquineau, S., Vargas, G. and Rutllant, J. a.: A
1131 simple model accounting for the uptake, transport, and deposition of wind-eroded mineral
1132 particles in the hyperarid coastal Atacama Desert of northern Chile, *Earth Surf. Process.*
1133 *Landforms*, 36(7), 923–932, doi:10.1002/esp.2122, 2011.

1134 An, F., Ma, H., Wei, H. and Lai, Z.: Distinguishing aeolian signature from lacustrine sediments
1135 of the Qaidam Basin in northeastern Qinghai-Tibetan Plateau and its palaeoclimatic implications,
1136 *Aeolian Res.*, 4, 17–30, doi:10.1016/j.aeolia.2011.12.004, 2012.

1137 Apaéstegui, J., Cruz, F. W., Sifeddine, a., Espinoza, J. C., Guyot, J. L., Khodri, M., Strikis, N.,
1138 Santos, R. V., Cheng, H., Edwards, L., Carvalho, E. and Santini, W.: Hydroclimate variability of
1139 the South American Monsoon System during the last 1600 yr inferred from speleothem isotope
1140 records of the north-eastern Andes foothills in Peru, *Clim. Past Discuss.*, 10(1), 533–561,
1141 doi:10.5194/cpd-10-533-2014, 2014a.

1142 Apaéstegui, J., Cruz, F. W., Sifeddine, A., Vuille, M., Espinoza, J. C., Guyot, J. L., Khodri, M.,
1143 Strikis, N. and Perú, G.: Hydroclimate variability of the northwestern Amazon Basin near the
1144 Andean foothills of Peru related to the South American Monsoon System during the last 1600
1145 years, *Clim. Past*, 10(1), 1967–1981, doi:10.5194/cp-10-1967-2014, 2014b.

1146 Bekaddour, T., Schlunegger, F., Vogel, H., Delunel, R., Norton, K. P., Akçar, N. and Kubik, P.:
1147 Paleo erosion rates and climate shifts recorded by Quaternary cut-and-fill sequences in the Pisco
1148 valley, central Peru, *Earth Planet. Sci. Lett.*, 390, 103–115, doi:10.1016/j.epsl.2013.12.048, 2014.

1149 Bendix, A., Bendix, J., Gämmerler, S., Reudenbach, C. and Weise, S.: The El Niño 1997 / 98 as
1150 seen from space - rainfall retrieval and investigation of rainfall dynamics with Goes-8 and TRMM
1151 Data, in *The 2002 EUMETSAT Meteor. Satellite Conf.*, Dublin, Ireland 02-06 Sept. 2002, EUM
1152 P 36, pp. 647–652., 2002.

1153 Bird, B. W., Abbott, M. B., Vuille, M., Rodbell, D. T., Stansell, N. D. and Rosenmeier, M. F.: A
1154 2,300-year-long annually resolved record of the South American summer monsoon from the
1155 Peruvian Andes., *Proc. Natl. Acad. Sci. U. S. A.*, 108(21), 8583–8,
1156 doi:10.1073/pnas.1003719108, 2011.

1157 Bloemsma, M. R., Zabel, M., Stuut, J. B. W., Tjallingii, R., Collins, J. a. and Weltje, G. J.:
1158 Modelling the joint variability of grain size and chemical composition in sediments, *Sediment.*
1159 *Geol.*, 280, 135–148, doi:10.1016/j.sedgeo.2012.04.009, 2012.

1160 Böning, P. and Brumsack, H.: Geochemistry of Peruvian near-surface sediments, *Geochim.*
1161 *Cosmochim. Acta*, 68(21), 4429–4451, doi:10.1016/j.gca.2004.04.027, 2004.

1162 Brodie, I. and Kemp, A. E. S.: Variation in Biogenic and Detrital Fluxes and Formation of
1163 Laminae in Late Quaternary Sediments from the Peruvian Coastal Upwelling Zone, *Mar. Geol.*,
1164 116(3-4), 385–398, doi:10.1016/0025-3227(94)90053-1, 1994.

1165 Chaigneau, A., Dominguez, N., Eldin, G., Vasquez, L., Flores, R., Grados, C. and Echevin, V.:
1166 Near-coastal circulation in the Northern Humboldt Current System from shipboard ADCP data,
1167 *J. Geophys. Res. Ocean.*, 118(10), 5251–5266, doi:10.1002/jgrc.20328, 2013.

- 1168 Ehlert, C., Grasse, P., Gutiérrez, D., Salvattecí, R. and Frank, M.: Nutrient utilisation and
1169 weathering inputs in the Peruvian upwelling region since the Little Ice Age, *Clim. Past*, 11, 187–
1170 202, doi:10.5194/cpd-10-3357-2014, 2015.
- 1171 England, M. H., McGregor, S., Spence, P., Meehl, G. a., Timmermann, A., Cai, W., Gupta, A.
1172 Sen, McPhaden, M. J., Purich, A. and Santoso, A.: Recent intensification of wind-driven
1173 circulation in the Pacific and the ongoing warming hiatus, *Nat. Clim. Chang.*, 4(3), 222–227,
1174 doi:10.1038/nclimate2106, 2014.
- 1175 Escobar Baccaro, D. F.: Evaluación climatológica y sinóptica del fenómeno de vientos Paracas,
1176 Universidad Nacional Agraria La Molina, Lima-Peru., 1993.
- 1177 Flores-Aqueveque, V., Alfaro, S. C., Caquineau, S., Foret, G., Vargas, G. and Rutllant, J. a.: Inter-
1178 annual variability of southerly winds in a coastal area of the Atacama Desert: implications for the
1179 export of aeolian sediments to the adjacent marine environment, *Sedimentology*, 59(3), 990–
1180 1000, doi:10.1111/j.1365-3091.2011.01288.x, 2012.
- 1181 Flores-Aqueveque, V., Alfaro, S., Vargas, G., Rutllant, J. a. and Caquineau, S.: Aeolian particles
1182 in marine cores as a tool for quantitative high-resolution reconstruction of upwelling favorable
1183 winds along coastal Atacama Desert, Northern Chile, *Prog. Oceanogr.*, 134, 244–255,
1184 doi:10.1016/j.pocean.2015.02.003, 2015.
- 1185 Garreaud, R. D. and Falvey, M.: The coastal winds off western subtropical South America in
1186 future climate scenarios, *Int. J. Climatol.*, 29(4), 543–554, doi:10.1002/joc.1716, 2009.
- 1187 Gay, S. P.: Blowing sand and surface winds in the Pisco to Chala Area, Southern Peru, *J. Arid
1188 Environ.*, 61(1), 101–117, doi:10.1016/j.jaridenv.2004.07.012, 2005.
- 1189 Gomes, L., Bergametti, G., Dulac, F. and Ezat, U.: Assessing the actual size distribution of
1190 atmospheric aerosols collected with a cascade impactor, *J. Aerosol Sci.*, 21(1), 47–59,
1191 doi:10.1016/0021-8502(90)90022-P, 1990.
- 1192 Gutiérrez, D., Bouloubassi, I., Sifeddine, A., Purca, S., Goubanova, K., Graco, M., Field, D.,
1193 Méjanelle, L., Velazco, F., Lorre, A., Salvattecí, R., Quispe, D., Vargas, G., Dewitte, B. and
1194 Ortlieb, L.: Coastal cooling and increased productivity in the main upwelling zone off Peru since
1195 the mid-twentieth century, *Geophys. Res. Lett.*, 38(7), 1–6, doi:10.1029/2010GL046324, 2011.
- 1196 Gutiérrez, D., Sifeddine, A., Field, D. B., Ortlieb, L., Vargas, G., Chávez, F., Velazco, F., Ferreira,
1197 V., Tapia, P., Salvattecí, R., Boucher, H., Morales, M. C., Valdés, J., Reyss, J.-L., Campusano,
1198 A., Boussafir, M., Mandeng-Yogo, M., García, M. and Baumgartner, T.: Rapid reorganization in
1199 ocean biogeochemistry off Peru towards the end of the Little Ice Age, *Biogeosciences Discuss.*,
1200 5(5), 3919–3943, doi:10.5194/bgd-5-3919-2008, 2008.
- 1201 Gutiérrez, D., Sifeddine, A., Field, D., Ortlieb, L., Vargas, G., Chaves, F., Velazco, F., Ferreira,
1202 V., Tapia, P., Salvattecí, R., Boucher, H., Morales, M. C., Valdes, J., Reyss, J., Campusano, A.,
1203 Boussafir, M., Mandeng-Yogo, M., Garcia, M. and Baumgartner, T.: Rapid reorganization in
1204 ocean biogeochemistry off Peru towards the end of the Little Ice Age, *Biogeosciences*, 6, 835–
1205 848, 2009.
- 1206 Gutiérrez, D., Sifeddine, A., Reyss, J., Vargas, G., Velasco, F., Salvattecí, R., Ferreira, V., Ortlieb,
1207 L., Field, D., Baumgartner, T., Boussafir, M., Boucher, H., Valdes, J., Marinovic, L., Soler, P.
1208 and Tapia, P.: Anoxic sediments off Central Peru record interannual to multidecadal changes of
1209 climate and upwelling ecosystem during the last two centuries., *Adv. Geosci.*, 6, 119–125, 2006.
- 1210 Haney, E. M. and Grolier, M. J.: Geologic map of major Quaternary eolian features, northern and
1211 central coastal Peru, *United States Geol. Surv. Misc. Investig.*, I-2162, 1991.
- 1212 Haug, G. H., Hughen, K. a, Sigman, D. M., Peterson, L. C. and Röhl, U.: Southward migration of
1213 the intertropical convergence zone through the Holocene., *Science*, 293(5533), 1304–8,
1214 doi:10.1126/science.1059725, 2001.

- 1215 Hesse, P. P. and McTainsh, G. H.: Last Glacial Maximum to Early Holocene Wind Strength in
1216 the Mid-latitudes of the Southern Hemisphere from Aeolian Dust in the Tasman Sea, *Quat. Res.*,
1217 52(3), 343–349, doi:10.1006/qres.1999.2084, 1999.
- 1218 Hill, E. A., Hickey, B. M., Shillington, F. A., Strub, P. T., Brink, K. H., Barton, E. D. and Thomas,
1219 A. C.: Eastern Ocean Boundaries coastal segment (E), in *The Sea*, Vol 11, vol. II, edited by A.
1220 Robinson and K. Brink, pp. 29–67, John Wiley & Sons Ltd., 1998.
- 1221 Holz, C., Stuut, J. B. W., Henrich, R. and Meggers, H.: Variability in terrigenous sedimentation
1222 processes off northwest Africa and its relation to climate changes: Inferences from grain-size
1223 distributions of a Holocene marine sediment record, *Sediment. Geol.*, 202(3), 499–508,
1224 doi:10.1016/j.sedgeo.2007.03.015, 2007.
- 1225 Huang, X., Oberhänsli, H., von Suchodoletz, H. and Sorrel, P.: Dust deposition in the Aral Sea:
1226 implications for changes in atmospheric circulation in central Asia during the past 2000 years,
1227 *Quat. Sci. Rev.*, 30(25-26), 3661–3674, doi:10.1016/j.quascirev.2011.09.011, 2011.
- 1228 Hyeong, K., Yoo, C. M., Kim, J., Chi, S.-B. and Kim, K.-H.: Flux and grain size variation of
1229 eolian dust as a proxy tool for the paleo-position of the Intertropical Convergence Zone in the
1230 northeast Pacific, *Palaeogeogr. Palaeoclimatol. Palaeoecol.*, 241(2), 214–223,
1231 doi:10.1016/j.palaeo.2006.03.011, 2006.
- 1232 Iversen, J. D. and White, B. R.: Saltation threshold on Earth, Mars and Venus, *Sedimentology*,
1233 29, 111–119, doi:10.1111/j.1365-3091.1982.tb01713.x, 1982.
- 1234 Kok, J. F., Parteli, E. J. R., Michaels, T. I. and Karam, D. B.: The physics of wind-blown sand
1235 and dust, *Reports Prog. Phys.*, 75(10), 106901, doi:10.1088/0034-4885/75/10/106901, 2012.
- 1236 Koopmann, B.: Sedimentation von Saharastaub im subtropischen Nordatlantik während der
1237 letzten 25.000 Jahre, *Meteor. Forsch. ergeb. R. C*, 35, 23–59, 1981.
- 1238 Lavado Casimiro, W., Ronchail, J., Labat, D., Espinoza, J. C. and Guyot, J. L.: Basin-scale
1239 analysis of rainfall and runoff in Peru (1969–2004): Pacific, Titicaca and Amazonas drainages,
1240 *Hydrol. Sci. J.*, 57(4), 625–642, doi:10.1080/02626667.2012.672985, 2012.
- 1241 Lavado-Casimiro, W. and Espinoza, J. C.: Impacts of El Nino and La Nina in the precipitation
1242 over Peru (1965-2007), *Rev. Bras. Meteorol.*, 29(2), 171–182, doi:10.1590/S0102-
1243 77862014000200003, 2014.
- 1244 Marticorena, B.: Dust Production Mechanisms, in *Mineral Dust: A Key Player in the Earth*
1245 *System*, edited by P. Knippertz and J.-B. Stuut, pp. 93–120, Springer, Dordrecht Heidelberg New
1246 York London., 2014.
- 1247 Marticorena, B. and Bergametti, G.: Modeling the atmospheric dust cycle: 1. Design of a soil-
1248 derived dust emission scheme, *J. Geophys. Res.*, 100(D8), 16415, doi:10.1029/95JD00690, 1995.
- 1249 McCave, I. N., Manighetti, B. and Robinson, S. G.: Sortable silt and fine sediment
1250 size/composition slicing: parameters for palaeocurrent speed and palaeoceanography,
1251 *Paleoceanography*, 10(3), 593–610, doi:10.1029/94PA03039, 1995.
- 1252 Mcgregor, S., Timmermann, A., Stuecker, M. F., England, M. H. and Merrifield, M.: Recent
1253 Walker circulation strengthening and Pacific cooling amplified by Atlantic warming, *Nat. Clim.*
1254 *Chang.*, (August), 1–5, doi:10.1038/NCLIMATE2330, 2014.
- 1255 McPhillips, D., Bierman, P. R., Crocker, T. and Rood, D. H.: Landscape response to Pleistocene-
1256 Holocene precipitation change in the Western Cordillera, Peru: 10 Be concentrations in modern
1257 sediments and terrace fills, *J. Geophys. Res. Earth Surf.*, 118(4), 2488–2499,
1258 doi:10.1002/2013JF002837, 2013.
- 1259 McTainsh, G. H., Nickling, W. G. and Lynch, a. W.: Dust deposition and particle size in Mali,
1260 West Africa, *Catena*, 29(3-4), 307–322, doi:10.1016/S0341-8162(96)00075-6, 1997.

- 1261 Meyer, I., Davies, G. R. and Stuut, J. B. W.: Grain size control on Sr-Nd isotope provenance
1262 studies and impact on paleoclimate reconstructions: An example from deep-sea sediments
1263 offshore NW Africa, *Geochemistry, Geophys. Geosystems*, 12(3), 14,
1264 doi:10.1029/2010GC003355, 2011.
- 1265 Molina-Cruz, A.: The relation of the southern trade winds to upwelling processes during the last
1266 75,000 years, *Quat. Res.*, 8(3), 324–338, doi:10.1016/0033-5894(77)90075-8, 1977.
- 1267 Montes, I., Colas, F., Capet, X. and Schneider, W.: On the pathways of the equatorial subsurface
1268 currents in the eastern equatorial Pacific and their contributions to the Peru-Chile Undercurrent,
1269 *J. Geophys. Res. Ocean.*, 115(9), 1–16, doi:10.1029/2009JC005710, 2010.
- 1270 Morera, S., Condom, T., Crave, A. and Galvez, C.: Tasas de erosión y dinámica de los flujos de
1271 sedimentos en la cuenca del río Santa , Perú, *Rev. Peru. Geo-Atmosférica RPGA*, 37(3), 25–37,
1272 2011.
- 1273 Oppo, D. W., Rosenthal, Y. and Linsley, B. K.: 2,000-year-long temperature and hydrology
1274 reconstructions from the Indo-Pacific warm pool., *Nature*, 460(7259), 1113–1116,
1275 doi:10.1038/nature08233, 2009.
- 1276 Ortlieb, L.: The Documented Historical Record of El Nino Events in Peru: An Update of the
1277 Quinn Record (Sixteenth through Nineteenth Centuries), in *El Nino and the Southern Oscillation,*
1278 *Multiscale Variability and Global and Regional Impacts*, pp. 207–295., 2000.
- 1279 Parkin, D. W. and Shackleton, N. .: Trade wind and temperature correlations down a deep sea
1280 core off the Sharan coast, *Nature*, 245, 455–457, 1973.
- 1281 Peterson, L. and Haug, G.: Variability in the mean latitude of the Atlantic Intertropical
1282 Convergence Zone as recorded by riverine input of sediments to the Cariaco Basin (Venezuela),
1283 *Palaeogeogr. Palaeoclimatol. Paleooceanogr.*, 234, 97–113, doi:10.1016/j.palaeo.2005.10.021,
1284 2006.
- 1285 Pichevin, L., Cremer, M., Giraudeau, J. and Bertrand, P.: A 190 ky record of lithogenic grain-size
1286 on the Namibian slope: Forging a tight link between past wind-strength and coastal upwelling
1287 dynamics, *Mar. Geol.*, 218(1-4), 81–96, doi:10.1016/j.margeo.2005.04.003, 2005.
- 1288 Prins, M.: Pelagic, hemipelagic and turbidite deposition in the Arabian Sea during the late
1289 Quaternary: Unravelling the signals of aeolian and fluvial sediment supply as functions of
1290 tectonics, sea-level and climate change by means of end-member modelling of silicic, Utrecht,
1291 Universiteit Utrecht., 1999.
- 1292 Prins, M. a., Vriend, M., Nugteren, G., Vandenberghe, J., Lu, H., Zheng, H. and Jan Weltje, G.:
1293 Late Quaternary aeolian dust input variability on the Chinese Loess Plateau: inferences from
1294 unmixing of loess grain-size records, *Quat. Sci. Rev.*, 26(1-2), 230–242,
1295 doi:10.1016/j.quascirev.2006.07.002, 2007.
- 1296 Quijano Vargas, J. J.: Estudio numerico y observacional de la dinámica de Viento Paracas,
1297 asociado al transporte eólico hacia el océano frente a la costa de Ica-Perú., Universidad Peruana
1298 Cayetano Heredia, Lima - Perú., 2013.
- 1299 Ratmeyer, V., Fischer, G. and Wefer, G.: Lithogenic particle fluxes and grain size distributions
1300 in the deep ocean off northwest Africa: Implications for seasonal changes of aeolian dust input
1301 and downward transport, *Deep Sea Res. Part I Oceanogr. Res. Pap.*, 46, 1289–1337, 1999.
- 1302 Rebesco, M., Hernández-Molina, F. J., Van Rooij, D. and Wåhlin, A.: Contourites and associated
1303 sediments controlled by deep-water circulation processes: State-of-the-art and future
1304 considerations, *Mar. Geol.*, 352, 111–154, doi:10.1016/j.margeo.2014.03.011, 2014.
- 1305 Rein, B.: El Niño variability off Peru during the last 20,000 years, *Paleoceanography*, 20(4),
1306 PA4003, doi:10.1029/2004PA001099, 2005.
- 1307 Rein, B.: How do the 1982/83 and 1997/98 El Niños rank in a geological record from Peru?, *Quat.*

- 1308 Int., 161(1), 56–66, doi:10.1016/j.quaint.2006.10.023, 2007.
- 1309 Rein, B., Lückge, A. and Sirocko, F.: A major Holocene ENSO anomaly during the Medieval
1310 period, *Geophys. Res. Lett.*, 31(17), L17211, doi:10.1029/2004GL020161, 2004.
- 1311 Reinhardt, L., Kudrass, H., Lückge, A., Wiedicke, M., Wunderlich, J. and Wendt, G.: High-
1312 resolution sediment echosounding off Peru Late Quaternary depositional sequences and
1313 sedimentary structures of a current-dominated shelf, *Mar. Geophys. Res.*, 23(1980), 335–351,
1314 2002.
- 1315 Reuter, J., Stott, L., Khider, D., Sinha, A., Cheng, H. and Edwards, R. L.: A new perspective on
1316 the hydroclimate variability in northern South America during the Little Ice Age, *Geophys. Res.*
1317 *Lett.*, 36(21), L21706, doi:10.1029/2009GL041051, 2009.
- 1318 Sachs, J. P., Sachse, D., Smittenberg, R. H., Zhang, Z., Battisti, D. S. and Golubic, S.: Southward
1319 movement of the Pacific intertropical convergence zone AD 1400–1850, *Nat. Geosci.*, 2(7), 519–
1320 525, doi:10.1038/ngeo554, 2009.
- 1321 Salvattecì, R., Field, D. B., Baumgartner, T., Ferreira, V. and Gutierrez, D.: Evaluating fish scale
1322 preservation in sediment records from the oxygen minimum zone off Peru, *Paleobiology*, 38(1),
1323 52–78, doi:10.1666/10045.1, 2012.
- 1324 Salvattecì, R., Field, D., Sifeddine, A., Ortlieb, L., Ferreira, V., Baumgartner, T., Caquineau, S.,
1325 Velazco, F., Reyss, J. L., Sanchez-Cabeza, J. A. and Gutierrez, D.: Cross-stratigraphies from a
1326 seismically active mud lens off Peru indicate horizontal extensions of laminae, missing sequences,
1327 and a need for multiple cores for high resolution records, *Mar. Geol.*, 357, 72–89,
1328 doi:10.1016/j.margeo.2014.07.008, 2014a.
- 1329 Salvattecì, R., Gutierrez, D., Field, D., Sifeddine, A., Ortlieb, L., Bouloubassi, I., Boussafir, M.,
1330 Boucher, H. and Cetin, F.: The response of the Peruvian Upwelling Ecosystem to centennial-scale
1331 global change during the last two millennia, *Clim. Past*, 10(1), 1–17, doi:10.5194/cp-10-1-2014,
1332 2014b.
- 1333 Salvattecì, R., Gutierrez, D., Sifeddine, A., Ortlieb, L., Druffel, E., Boussafir, M. and Schneider,
1334 R.: Centennial to millennial-scale changes in oxygenation and productivity in the Eastern Tropical
1335 South Pacific during the last 25,000 years, *Quat. Sci. Rev.*, 131, 102–117,
1336 doi:10.1016/j.quascirev.2015.10.044, 2016.
- 1337 Saukel, C., Lamy, F., Stuut, J. B. W., Tiedemann, R. and Vogt, C.: Distribution and provenance
1338 of wind-blown SE Pacific surface sediments, *Mar. Geol.*, 280(1-4), 130–142,
1339 doi:10.1016/j.margeo.2010.12.006, 2011.
- 1340 Scheidegger, K. F. and Krissek, L. A.: Dispersal and deposition of eolian and fluvial sediments
1341 off Peru and northern Chile., *Geol. Soc. Am. Bull.*, 93(2), 150–162, doi:10.1130/0016-
1342 7606(1982)93<150:DADDOEA>2.0.CO;2, 1982.
- 1343 Schweigger, E.: *El litoral peruano (Segunda edición)*., Lima: Universidad Nacional “Federico
1344 Villarreal”, 1964., 1984.
- 1345 Sears, M.: Notes on the Peruvian coastal current. 1. An introduction to the ecology of Pisco Bay,
1346 *Deep Sea Res.*, 1(3), 141–169, doi:10.1016/0146-6313(54)90045-3, 1954.
- 1347 Shao, Y., Ishizuka, M., Mikami, M. and Leys, J. F.: Parameterization of size-resolved dust
1348 emission and validation with measurements, *J. Geophys. Res. Atmos.*, 116(January), 1–19,
1349 doi:10.1029/2010JD014527, 2011.
- 1350 Shao, Y. and Lu, H.: A simple expression for wind erosion threshold friction velocity, *J. Geophys.*
1351 *Res.*, 105(d), 22437, doi:10.1029/2000JD900304, 2000.
- 1352 Sifeddine, A., Gutiérrez, D., Ortlieb, L., Boucher, H., Velazco, F., Field, D., Vargas, G.,
1353 Boussafir, M., Salvattecì, R., Ferreira, V., García, M., Valdés, J., Caquineau, S., Mandeng Yogo,
1354 M., Cetin, F., Solis, J., Soler, P. and Baumgartner, T.: Laminated sediments from the central

- 1355 Peruvian continental slope: A 500 year record of upwelling system productivity, terrestrial runoff
1356 and redox conditions, *Prog. Oceanogr.*, 79(2-4), 190–197, doi:10.1016/j.pocean.2008.10.024,
1357 2008.
- 1358 Smith, R. L.: Circulation patterns in upwelling regimes, *Coast. upwelling*, 13–35, 1983.
- 1359 Strub, P. T., Mesías, J. M. J. M., Montecino, V., Rutllant, J. A., Salinas, S., Robinson, A. R. and
1360 Brink, K. H.: Coastal ocean circulation off western South America, in *The Sea*, vol. 11, pp. 273–
1361 313., 1998.
- 1362 Stuut, J. W., Prins, M. A. and Weltje, G. J.: The palaeoclimatic record provided by aeolian dust
1363 in the deep sea: proxies and problems, *Geophys. Res. Abstr.*, 7, 10886, doi:1607-
1364 7962/gra/EGU05-A-10886, 2005.
- 1365 Stuut, J.-B. W., Kasten, S., Lamy, F. and Hebbeln, D.: Sources and modes of terrigenous sediment
1366 input to the Chilean continental slope, *Quat. Int.*, 161(1), 67–76,
1367 doi:10.1016/j.quaint.2006.10.041, 2007.
- 1368 Stuut, J.-B. W. and Lamy, F.: Climate variability at the southern boundaries of the Namib
1369 (southwestern Africa) and Atacama (northern Chile) coastal deserts during the last 120,000 yr,
1370 *Quat. Res.*, 62(3), 301–309, doi:10.1016/j.yqres.2004.08.001, 2004.
- 1371 Stuut, J.-B. W., Prins, M. a., Schneider, R. R., Weltje, G. J., Jansen, J. H. F. and Postma, G.: A
1372 300-kyr record of aridity and wind strength in southwestern Africa: inferences from grain-size
1373 distributions of sediments on Walvis Ridge, SE Atlantic, *Mar. Geol.*, 180(1-4), 221–233,
1374 doi:10.1016/S0025-3227(01)00215-8, 2002.
- 1375 Suess, E., Kulm, L. D. and Killingley, J. S.: Coastal upwelling and a history of organic-rich
1376 mudstone deposition off Peru, *Geol. Soc. London, Spec. Publ.*, 26(1), 181–197,
1377 doi:10.1144/GSL.SP.1987.026.01.11, 1987.
- 1378 Sun, D., Bloemendal, J., Rea, D. ., Vandenberghe, J., Jiang, F., An, Z. and Su, R.: Grain-size
1379 distribution function of polymodal sediments in hydraulic and aeolian environments, and
1380 numerical partitioning of the sedimentary components, *Sediment. Geol.*, 152(3-4), 263–277,
1381 doi:10.1016/S0037-0738(02)00082-9, 2002.
- 1382 Sydeman, W. J., García-Reyes, M., Schoeman, D. S., Rykaczewski, R. R., Thompson, S. a, Black,
1383 B. a and Bograd, S. J.: Climate change and wind intensification in coastal upwelling ecosystems.,
1384 *Science*, 345(6192), 77–80, doi:10.1126/science.1251635, 2014.
- 1385 Timmermann, A., Okumura, Y., An, S. I., Clement, a., Dong, B., Guilyardi, E., Hu, a., Jungclaus,
1386 J. H., Renold, M., Stocker, T. F., Stouffer, R. J., Sutton, R., Xie, S. P. and Yin, J.: The influence
1387 of a weakening of the Atlantic meridional overturning circulation on ENSO, *J. Clim.*, 20(19),
1388 4899–4919, doi:10.1175/JCLI4283.1, 2007.
- 1389 Unkel, I., Kadereit, A., Mächtle, B., Eitel, B., Kromer, B., Wagner, G. and Wacker, L.: Dating
1390 methods and geomorphic evidence of palaeoenvironmental changes at the eastern margin of the
1391 South Peruvian coastal desert (14°30'S) before and during the Little Ice Age, *Quat. Int.*, 175(1),
1392 3–28, doi:10.1016/j.quaint.2007.03.006, 2007.
- 1393 Weltje, G. J.: End-member modeling of compositional data: Numerical-statistical algorithms for
1394 solving the explicit mixing problem, *Math. Geol.*, 29(4), 503–549, doi:10.1007/BF02775085,
1395 1997.
- 1396 Weltje, G. J. and Prins, M. a: Muddled or mixed? Inferring palaeoclimate from size distributions
1397 of deep-sea clastics, *Sediment. Geol.*, 162(1-2), 39–62, doi:10.1016/S0037-0738(03)00235-5,
1398 2003.
- 1399 Weltje, G. J. and Prins, M. a.: Genetically meaningful decomposition of grain-size distributions,
1400 *Sediment. Geol.*, 202(3), 409–424, doi:10.1016/j.sedgeo.2007.03.007, 2007.
- 1401 Wentworth, C. K.: A Scale of Grade and Class Terms for Clastic Sediments, *J. Geol.*, 30(5), 377–

1402 392, doi:10.1086/622910, 1922.

1403

1404

1405

1406

1407

1408

1409
1410
1411
1412
1413
1414
1415
1416
1417
1418

Table 1: Averaged parameters (geometric mean diameter (Gmd), amplitude (A) and geometric standard deviation (Gsd)) of the 4 log-normal modes (components) identified from measured size distributions of sediment samples (B6 and G10 cores).

<u>M1</u>			<u>M2</u>			<u>M3</u>			<u>M4</u>		
<u>Gmd</u> <u>(μm)</u>	<u>A (%)</u>	<u>Gsd</u>	<u>Gmd</u> <u>(μm)</u>	<u>A (%)</u>	<u>Gsd</u>	<u>Gmd</u> <u>(μm)</u>	<u>A (%)</u>	<u>Gsd</u>	<u>Gmd</u> <u>(μm)</u>	<u>A (%)</u>	<u>Gsd</u>
<u>3 ± 1</u>	<u>16 ± 7</u>	<u>1.9 ± 0.2</u>	<u>10 ± 2</u>	<u>43 ± 15</u>	<u>1.9 ± 0.2</u>	<u>54 ± 12</u>	<u>20 ± 10</u>	<u>1.4 ± 0.2</u>	<u>90 ± 13</u>	<u>20 ± 13</u>	<u>1.2 ± 0.2</u>

1419

Table 21. Minimum, maximum and average values to the grain size components in each unit obtained along the record in the Pisco continental shelf.

1420

1421

1422

1423

1424

1425

1426

1427

1428

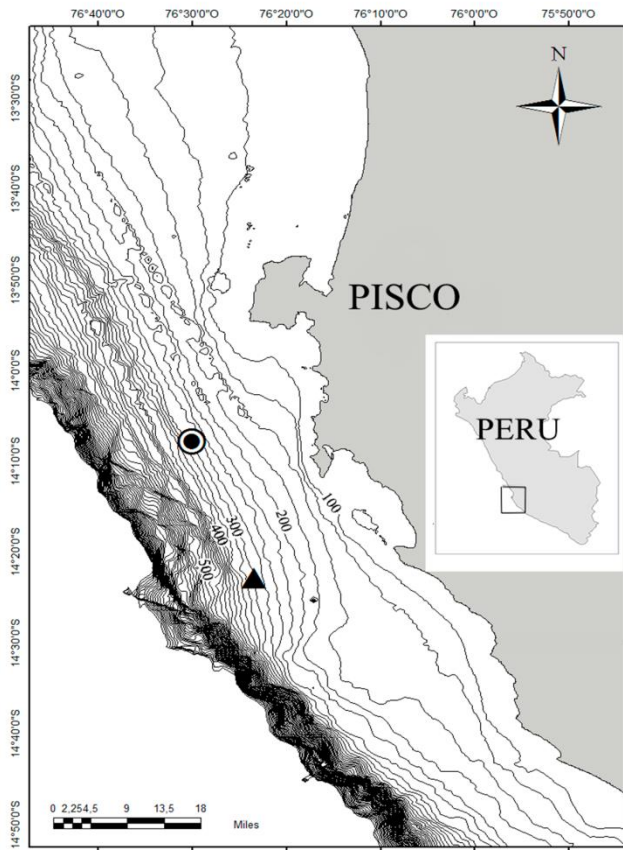
1429

1430

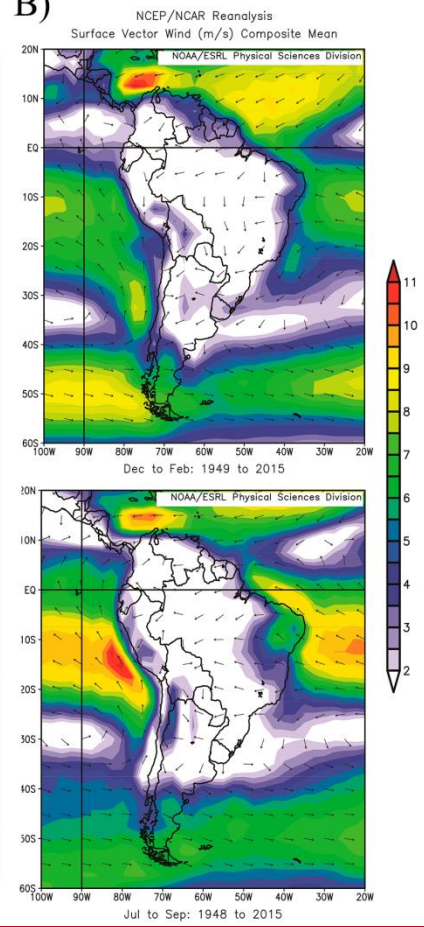
1431

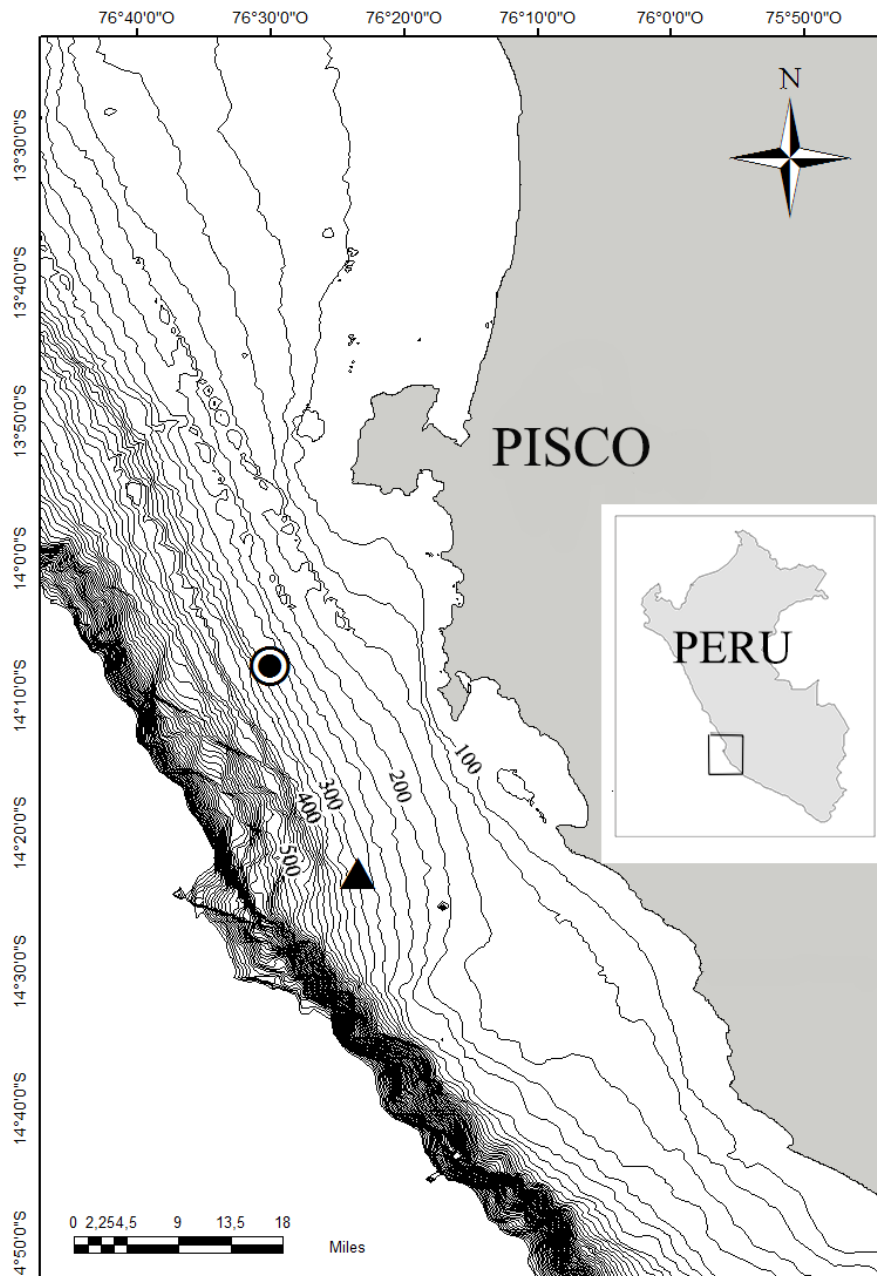
	First period MCA		Second period MCA		LIA		CWP	
	900 – 1170 A.D.		1170 – 1450A.D.		1450 – 1800 A.D.		1900 A.D to present	
Grain size	dV/dlnd (%)		dV/dlnd (%)		dV/dlnd (%)		dV/dlnd (%)	
componens	Av/Std.Dv.	Range (Min.-Max.)	Av/Std.Dv.	Range (Min.-Max.)	Av/Std.Dv.	Range (Min.-Max.)	Av/Std.Dv.	Range (Min.-Max.)
M1	11 ± 4	7 - 19	14 ± 6,0	5 - 27	15 ± 6	6 - 29	18 ± 7	4 - 40
M2	50 ± 10	33 - 64	41 ± 10	23 - 62	53 ± 15	16 - 80	34 ± 10	13 - 63
M3	18 ± 7	6 - 28	21 ± 9	0 - 39	19 ± 9	4 - 45	23 ± 10	6 - 44
M4	21 ± 8	8 - 42	24 ± 15	0 - 55	14 ± 11	0 - 44	25 ± 13	0 - 56

A)



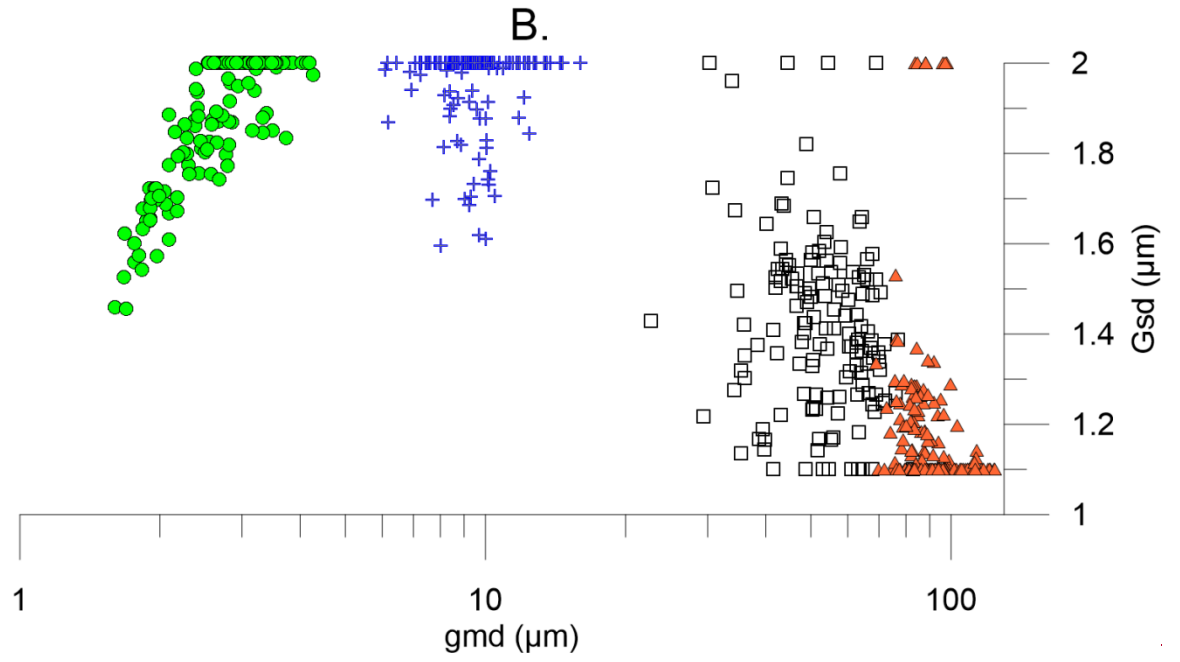
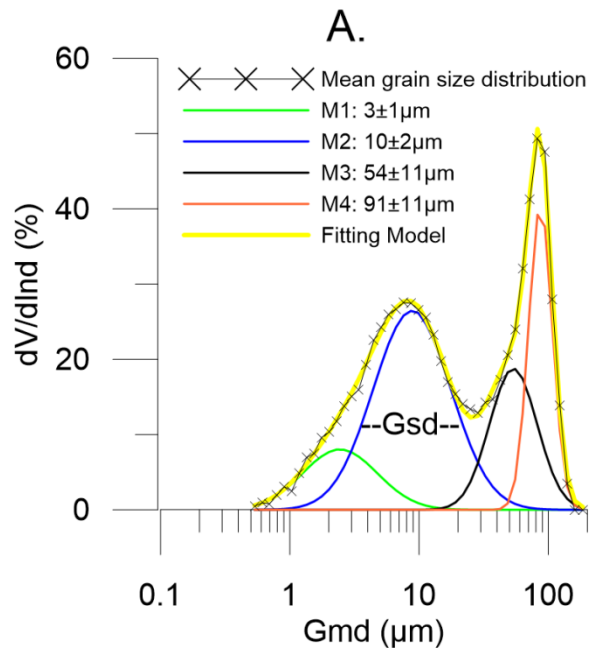
B)

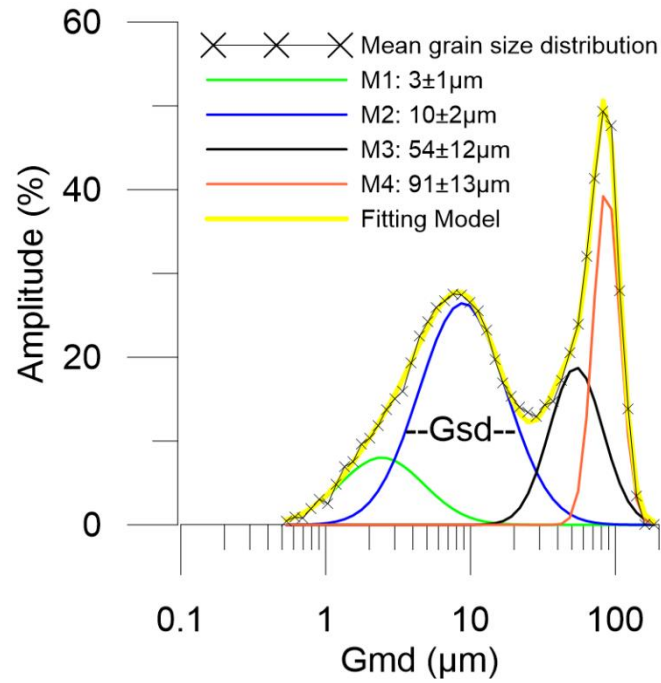




1433

1434 Figure 1. A) Location of the sampling of the sediment cores B040506 (black circle) and
 1435 G10-GC-01(black triangle) in the Central Peru continental margin. Bathymetric contour
 1436 lines are in 25m intervals from 100m to 500 m depth. B) Mean surface vector wind
 1437 velocity (m/s) composite mean for summer (up) and winter (down) between 1948 and
 1438 2015 at South American. NCEP/NCAR Reanalysis data.Location of the sampling of the
 1439 sediment cores B040506 (black circle) and G10-GC-01(black triangle) in the Central Peru
 1440 continental margin. Bathymetric contour lines are in 25m intervals from 100m to 500 m depth.





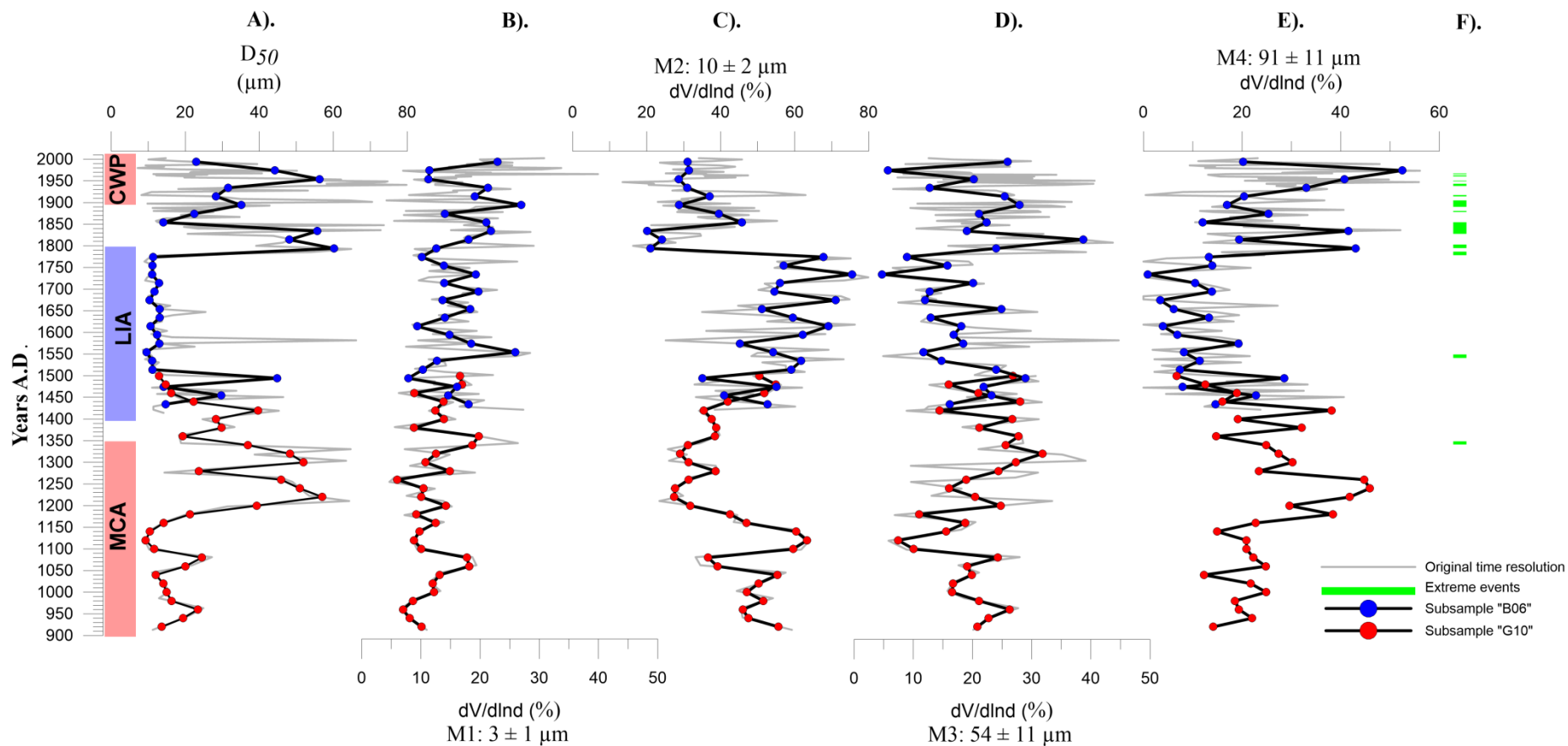
1443

1444 ~~Figure 2. A) Description of the four modes fitted calculates (M1, M2, M3 and M4) for the mean grain size of the total record; in detail is showed an example of~~
 1445 ~~geometrical standard deviation (Gsd) and its frequency (dV/dln d (%)) and B) The Gsd and geometrical mean diameter (Gmd) plotted of the unmixed components.~~

1446 Figure 2: Comparison between a measured grain size distribution and the fitted curve using log-normal function and its partitioning into four individual grain
 1447 size modes. The measured data is a mean grain-size distribution from all samples of B6 and G10 cores.

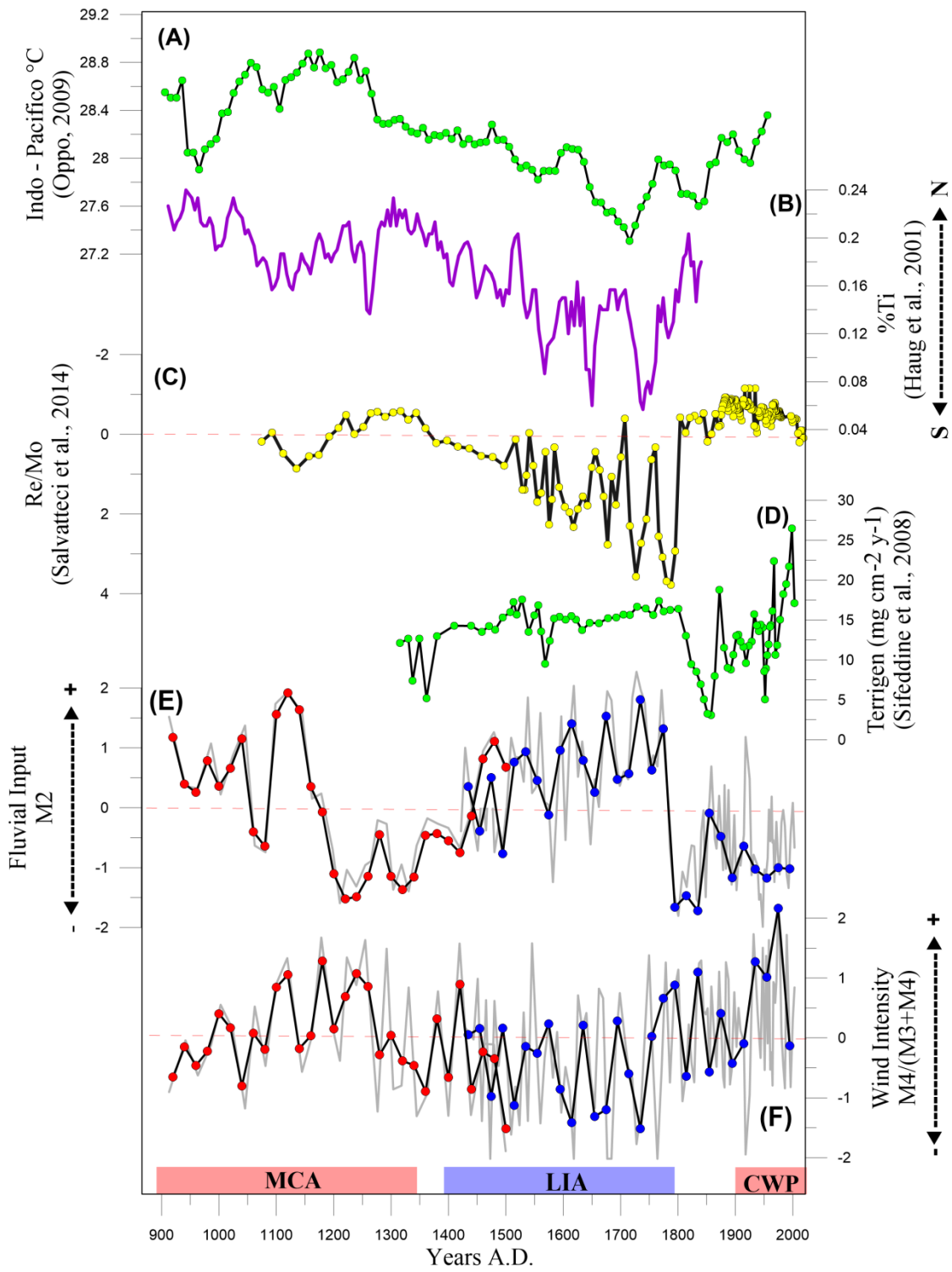
1448

1449



1450

1451 Figure 3. A) The median grain size (D50) variation along the record and variation in relative abundance of the sedimentary components: B) M1, C) Fluvial
 1452 (M2), D) Aeolian (M3) and E) Aeolian (M4) of the grain size distribution in the record F) Represent the samples where was found very large particles related
 1453 with extreme events.



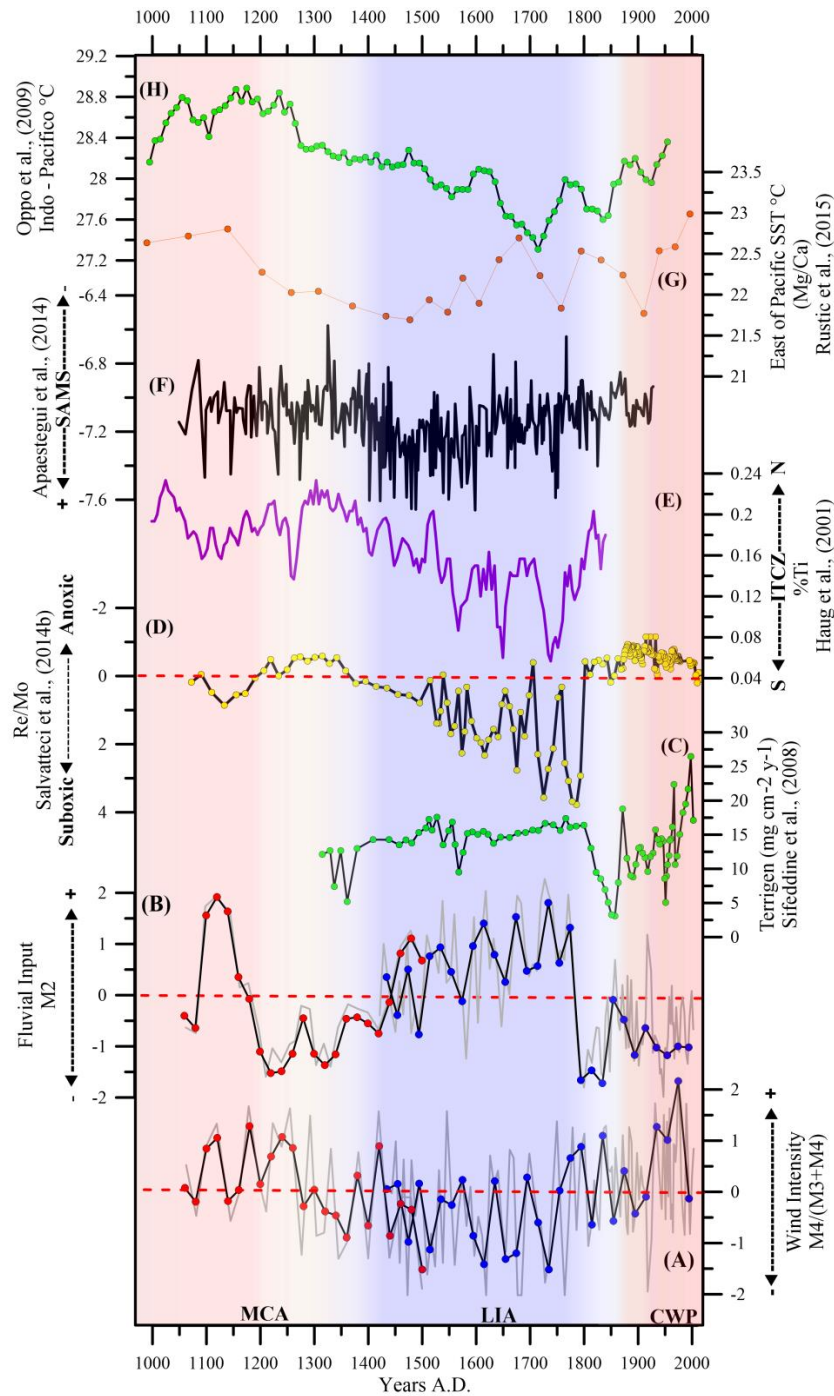


Figure 4. Reconstruction of A) Indo-Pacific temperatures reconstruction (Oppo et al., 2009), B) ITCZ migration (%Ti) (Peterson and Haug, 2006), C) OMZ activity (Re/Mo anomalies) negative values indicate more anoxic conditions (the axis was reversed) (Salvatteci et al., 2014b), D) Terrigenous flux (total minerals) in Pisco continental shelf by Sifeddine et al (2008), E) Fluvial input (M2) anomaly reconstruction on the continental shelf, F) Wind intensity (M4/(M3+M4)) anomaly reconstruction. A) Wind intensity (M4/(M3+M4)) anomaly reconstruction, B) Fluvial input (M2) anomaly reconstruction on the continental shelf, and records of C) Terrigenous flux (total minerals) in Pisco continental shelf

by Sifeddine et al (2008), D) OMZ activity (Re/Mo anomalies) negative values indicate more anoxic conditions (the axis was reversed) (Salvatteci et al., 2014b), E) ITCZ migration (%Ti) (Peterson and Haug, 2006), F) SAMS activity reconstruction ($\delta^{18}\text{O}$ Palestina Cave) (Apaéstegui et al., 2014), G) Indo-Pacific temperatures reconstruction (Oppo et al., 2009).

Supplementary Information:

Stacked record.

According to Salvatceci et al (2014), the cross-correlation of stratigraphic laminated sequences involves the identification of common biogeochemical features in the cores compared of the same study area. The common biogeochemical features are used as a correlation point between these. The biogeochemical shift at AD 1820±15 described by Gutiérrez et al., (2009) and Sifeddine et al., (2008) in all sediment cores in the area was used as stratigraphic anchored. Thereafter a visual examination of the X-ray images was made to prepare a correlation following the tone patterns produced by the difference in density of the laminae. The sediment core B14 (collected in the Pisco continental shelf too) was used as reference because this core were better defined and have most complete laminar sequence and is the best preserved (Figure 1S).

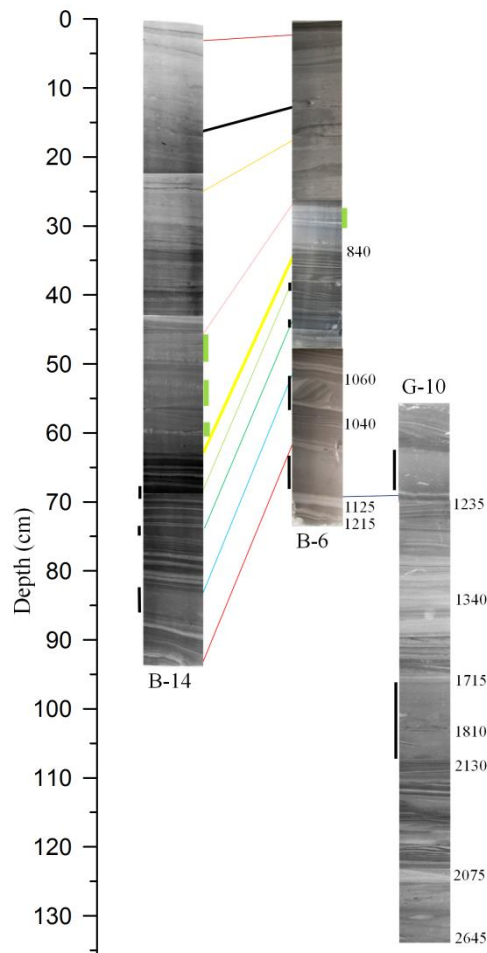


Figure 1S: Cross-correlation of stratigraphic laminated sequences (SCOPIX images) between the box core B14 (the undisturbed, and well-preserved laminae sequences), B6 and the gravity core G10 all retrieved in Pisco continental shelf. The SCOPIX images the colors were inverted, thus the darker (lighter) laminae represent dense (less dense) sediments. The numbers at the right side of the images represent the uncalibrated ^{14}C ages. Yellow line indicate the position of the sedimentological/biogeochemical shift (Gutiérrez et al., 2009). The upper black bold line indicates the start of ^{241}Am activity. The Black bars at the left side of the cores indicate homogeneous deposits, while green bars at the right side indicate the extent of the diatom layers. The stratigraphic markers are represented by the continuous colored thin lines that indicate possible (less obvious) correlations, methodology details in Salvattecí et al., (2014).

Downcore profile of excess ^{210}Pb and ^{241}Am in the Pisco boxcore B040506

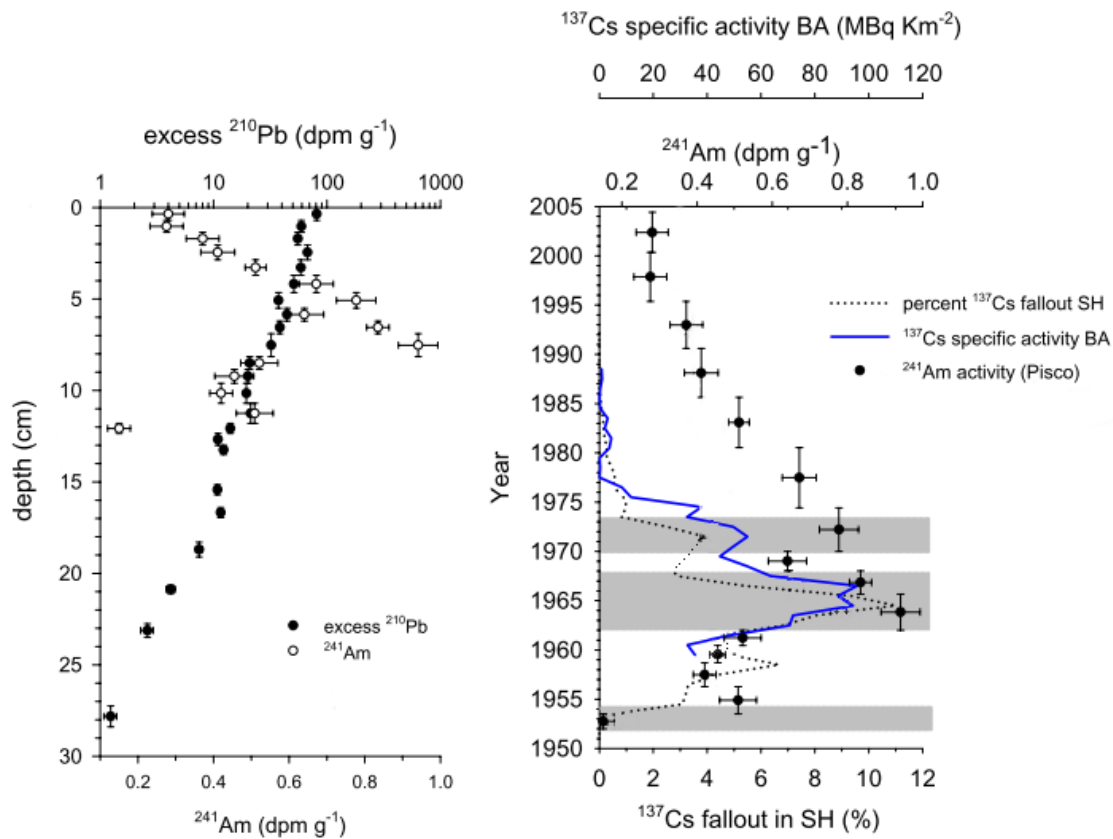


Figure 2S: Downcore profile of excess ^{210}Pb and ^{241}Am in the Pisco boxcore B040506. Reconstructed fallout of ^{137}Cs in the Southern Hemisphere (UNSCEAR, 2000), and fallout specific activity of ^{137}Cs in Buenos Aires (Ribeiro & Arribére, 2002). The prominent features of fallout change (onset and peak periods, shaded) were used to identify three time-markers in the downcore ^{241}Am specific activity for both cores. Time intervals for each time-marker were estimated from excess ^{210}Pb – derived sedimentation rate in the uppermost layer and sample layer thickness (taken and modified from Gutiérrez et al., (2009)).

Record of the entire grain size distribution.

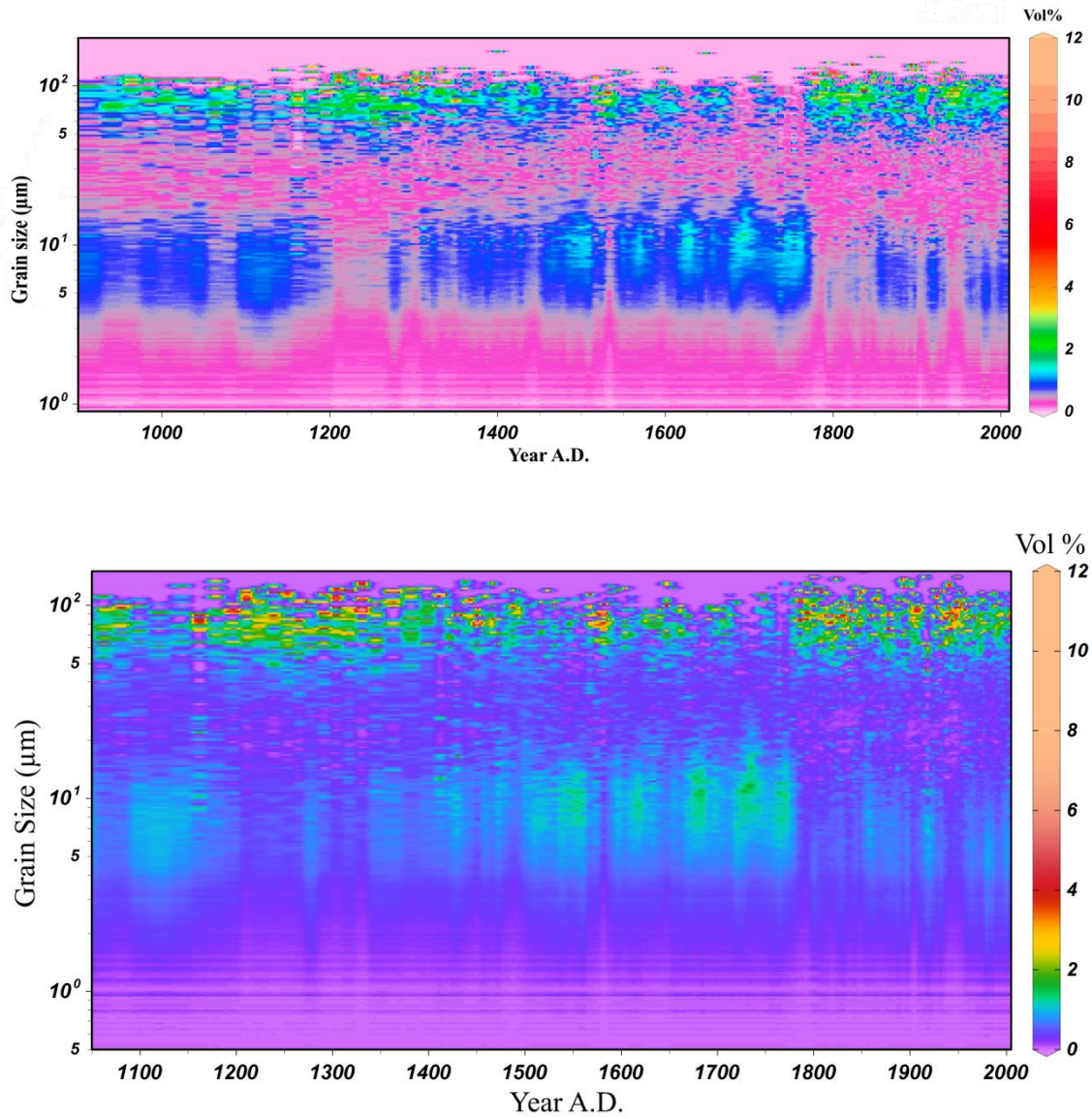


Figure 3S **Figure 1S**: Grain-size data distribution corresponding to the entire record (overlapping of the B040506 and G10-GC-01 sediment core). Two modes of grain sizes are apparent. A first one with finest grains range from ~2 to 15 µm; and the second one with coarser grains varied between of ~50-120 µm.

Principal component analysis of grain size classification.

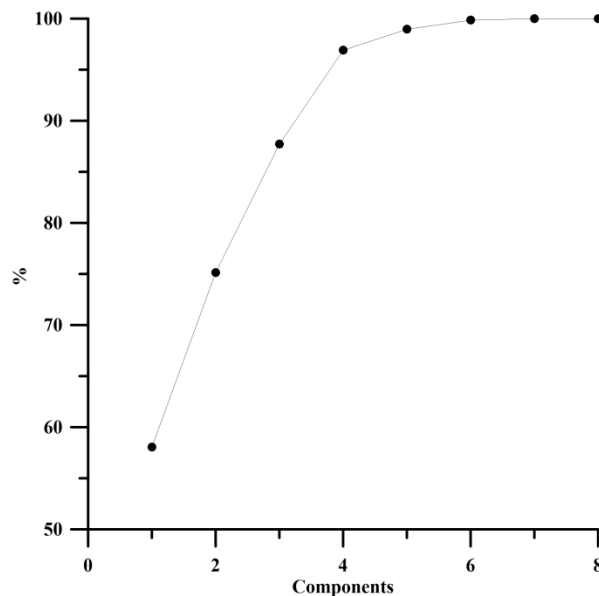


Figure 4S ~~Figure 2S~~: Variability proportion (coefficient of determination) obtained by principal components analysis (PCA) based on grain-size classification of Wentworth (1922). Four components can explain 97% of the total variability of the samples.

Supplementary Bibliography

Gutiérrez, D., Sifeddine, A., Field, D., Ortlieb, L., Vargas, G., Chaves, F., Velazco, F., Ferreira, V., Tapia, P., Salvattecí, R., Boucher, H., Morales, M. C., Valdes, J., Reyss, J., Campusano, A., Boussafir, M., Mandeng-Yogo, M., García, M. and Baumgartner, T.: Rapid reorganization in ocean biogeochemistry off Peru towards the end of the Little Ice Age, *Biogeosciences*, 6, 835–848, 2009.

Salvattecí, R., Field, D., Sifeddine, A., Ortlieb, L., Ferreira, V., Baumgartner, T., Caquineau, S., Velazco, F., Reyss, J. L., Sanchez-Cabeza, J. A. and Gutierrez, D.: Cross-stratigraphies from a seismically active mud lens off Peru indicate horizontal extensions of laminae, missing sequences, and a need for multiple cores for high resolution records, *Mar. Geol.*, 357, 72–89, doi:10.1016/j.margeo.2014.07.008, 2014.

Sifeddine, A., Gutiérrez, D., Ortlieb, L., Boucher, H., Velazco, F., Field, D., Vargas, G., Boussafir, M., Salvattecí, R., Ferreira, V., García, M., Valdés, J., Caquineau, S., Mandeng Yogo, M., Cetin, F., Solis, J., Soler, P. and Baumgartner, T.: Laminated sediments from the central Peruvian continental slope: A 500 year record of upwelling system productivity, terrestrial runoff and redox conditions, *Prog. Oceanogr.*, 79(2-4), 190–197, doi:10.1016/j.pcean.2008.10.024, 2008.

Wentworth, C. K.: A Scale of Grade and Class Terms for Clastic Sediments, *J. Geol.*, 30(5), 377–392, doi:10.1086/622910, 1922.